Structural Details of Human Aquaporin Regulation

Three stories of three aquaporins

Nesverova, Veronika

2020

Document Version:
Publisher's PDF, also known as Version of record

Structural Details of Human Aquaporin Regulation

VERONIKA NESVEROVA | BIOCHEMISTRY AND STRUCTURAL BIOLOGY | LUND UNIVERSITY

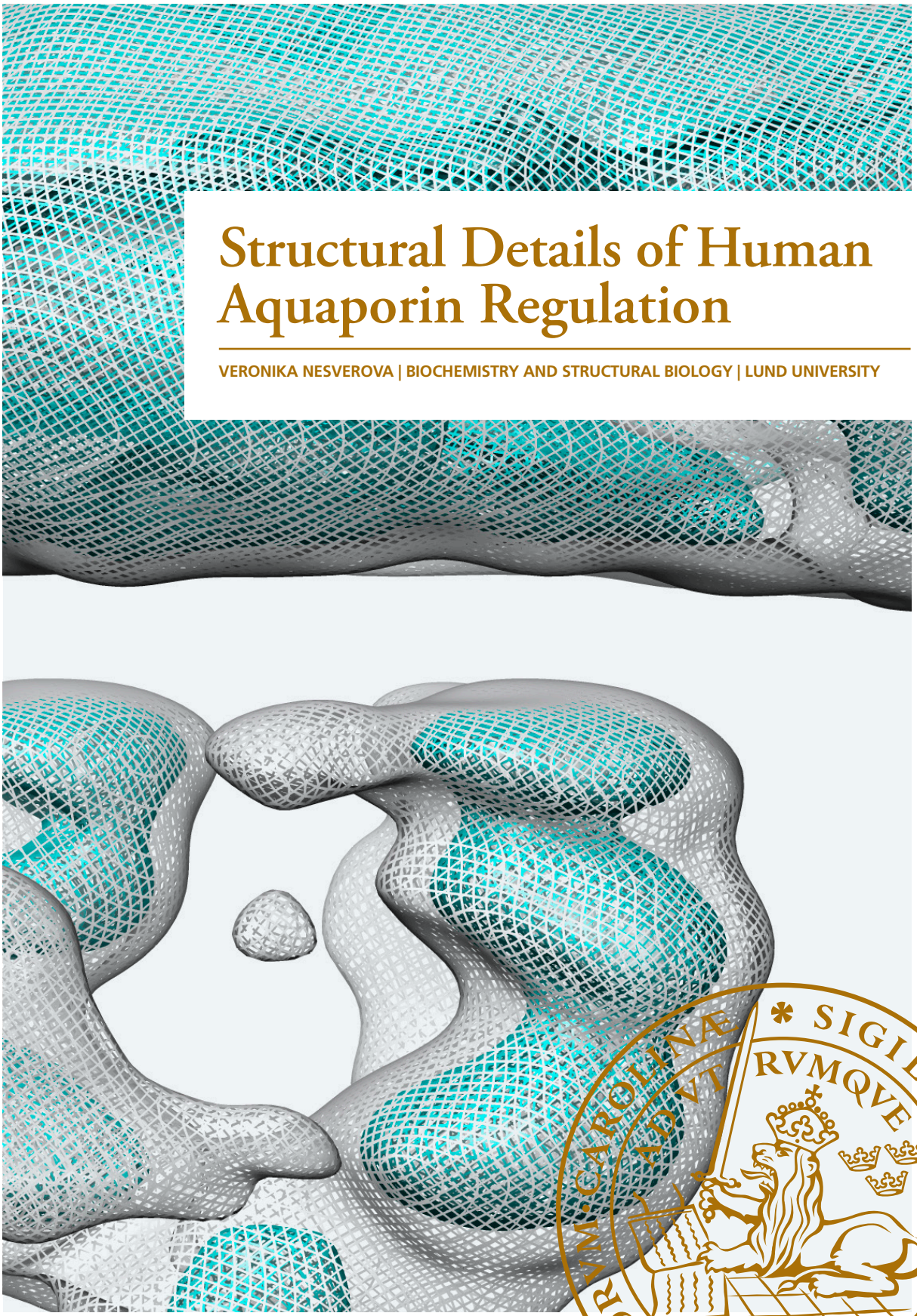

Structural Details of Human Aquaporin Regulation

Structural Details of Human Aquaporin Regulation

Three stories of three aquaporins

Veronika Nesverova

LUND
UNIVERSITY

DOCTORAL DISSERTATION
by due permission of the Faculty of Science, Lund University, Sweden.
To be defended on 28th February 2020 at 9:15 in Hall C, Kemicentrum

Faculty opponent
Prof. Christine Ziegler
University of Regensburg, Germany

Organization LUND UNIVERSITY	Document name: Doctoral Dissertation
Division of Biochemistry and Structural Biology	Date of issue: 2020-02-04
Author: Veronika Nesverova	Sponsoring organization

Title and subtitle: Structural Details of Human Aquaporin Regulation – Three stories of three aquaporins

Abstract:

Every cell is surrounded by a thin plasma membrane, protecting it from its surrounding. Specialized protein channels and transporters are embedded in this membrane, ensuring selective transport of molecules in and out of the cells. To maintain optimal hydration, water channels called aquaporins (AQPs) are present in every cell of our body. Thirteen isoforms of aquaporins exist in humans of which three, AQP2, AQP5 and AQP0, were studied in this thesis. The water passage through aquaporins needs to be very tightly regulated which happens by two distinct post-translational mechanisms. Either, the protein can be trafficked to the plasma membrane from storage vesicles when needed, like the case of AQP2 and AQP5. Alternatively, the channel might open and close based on the needs of the cell, which is a preferred way of regulation for AQP0. The need for regulation is signaled by a trigger – for example by changes in osmolarity and pH or by a hormone binding to its receptor. This signal is then carried out by binding to other regulatory proteins and/or by post-translational modifications, specifically phosphorylation.

In this thesis we studied the structural details of three protein-protein interactions involved in regulation of human AQP2, AQP5 and AQP0 by trafficking or gating. The binding of AQP2 to lysosomal trafficking regulator-interacting protein 5 (LIP5) targets AQP2 to multivesicular bodies of the endosomal sorting pathway. We quantified the effect of phosphorylation on this interaction using microscale thermophoresis (MST) and we studied the binding interface using molecular docking, mutational studies and fluorescence quenching. Our results reveal that LIP5 binds AQP2 in a same way as it binds the ESCRT-III complex of the endosomal sorting machinery. We have identified residues important for the interaction and showed that AQP2 phosphorylation at specific sites located outside the LIP5 binding site impairs the binding to LIP5. Moreover, we have obtained an 8Å cryo-EM model of the complex in a phospholipid nanodisc, which confirms our previous results and shows that two molecules of LIP5 bind each AQP2 tetramer. This structure and the method used to obtain it serve as a stepping stone towards structure determination of other aquaporin complexes.

For AQP5, the interaction with prolactin-inducible protein (PIP) is suggested to be important for its trafficking to the plasma membrane. We have characterized the interaction between the full-length proteins using MST and showed that it is mediated by the distal C-terminus and that one PIP molecule binds the AQP5 tetramer. In case of AQP0, the binding of calmodulin (CaM) upon increased intracellular calcium concentrations closes the channel. Using MST and a liposome-based water permeability assay, we showed that binding of CaM is inhibited by AQP0 phosphorylation at two different sites but that phosphorylation of a third site allows CaM to bind in a manner that keeps the channel open.

Our studies give new insights into the role of protein-protein interactions and phosphorylation in two distinct AQP regulatory mechanisms, thereby significantly increasing our understanding of how cellular water permeability can be controlled in a tissue-dependent manner.

Keywords: aquaporins, aquaporin regulation, protein-protein interaction, protein phosphorylation, cryo-EM, aquaporin 2, aquaporin 5, aquaporin 0, water channels, protein trafficking, membrane proteins

Classification system and/or index terms (if any)

Supplementary bibliographical information		Language: English
ISSN and key title		ISBN: Print 978-91-7422-724-6 Digital 978-91-7422-725-3
Recipient's notes	Number of pages: 81	Price
	Security classification	

Signature 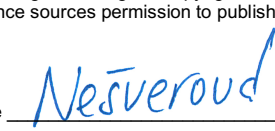 Date 2020-01-15

Structural Details of Human Aquaporin Regulation

Three stories of three aquaporins

Veronika Nesverova

LUND
UNIVERSITY

Cover image by Veronika Nesverova

Faculty of Science
Division of Biochemistry and Structural Biology

ISBN Print: 978-91-7422-724-6
ISBN Digital: 978-91-7422-725-3

Printed in Sweden by Media-Tryck, Lund University
Lund 2020

To society

May this work help to increase the quality of life of many,
somewhere down the road.

Table of Contents

Popular summary

An average human cell contains around 1 billion of protein molecules of 20 000 different types. These proteins are not only the building material and the muscles that hold our bodies upright and allows us to move, but they are also absolutely crucial for all our bodily functions – from digestion, fighting off infections, signalling hunger to the brain, to feeling loved.

One critical bodily function is the ability to keep hydrated. The movement of water in and out of the cells is very tightly regulated, making sure that all the cells contain just enough of the water they need but not too much. To ensure this, there are specialized proteins called aquaporins which function as small channels and that allow water to go in and out of the cells. Without these channels this would be very difficult because the cells are wrapped by a lipid membrane, a barrier that protects them from the outside environment and that limits the passage of water.

Three slightly different kinds of aquaporins were studied in this thesis. Aquaporin 0 which can be found in the eye lens, aquaporin 5 that is responsible for producing tears and saliva and aquaporin 2 which reabsorbs some of the water that our kidneys filter out from blood and therefore regulates the urine volume. However, in these projects we did not touch the human body at all. Instead we taught (genetically modified) bacteria and yeast to produce the particular human protein, which we then isolated and studied in a test tube.

Aquaporins are never alone since the cell is very crowded, full of different other kinds of proteins. This is important because when two or more proteins connect this often changes their function. Such protein-protein interactions and small chemical protein modifications decide the destiny of aquaporins – whether they will be open for water or closed, whether they will be present in the cell membrane, moved inside the cell for storage or degraded. In this thesis we measured how strong the interactions are and how small changes in the protein structure affect the binding. We also took a look at the overall structure of one of the protein-protein complexes with an electron microscope.

The results presented here contribute as one piece of puzzle into the big picture of how optimal hydration is maintained by the human body. Understanding these detailed processes of changes in structure and therefore in function could help us prevent or treat various conditions like the disease of reduced ability to concentrate urine (nephrogenic diabetes insipidus), the dry eye syndrome or cataract.

List of publications

Paper I — Roche, J. V.; Survery, S.; Kreida, S.; **Nesverova, V.**; Ampah-Korsah, H.; Gourdon, M.; Deen, P. M. T.; Törnroth-Horsefield, S. *Phosphorylation of Human Aquaporin 2 (AQP2) Allosterically Controls Its Interaction with the Lysosomal Trafficking Protein LIP5.* J. Biol. Chem. 2017, *292* (35), 14636–14648.

Paper II — Roche, J. V.*; **Nesverova, V.***; Olsson, C.; Deen, P. M. T.; Törnroth-Horsefield, S. *Structural Insights into AQP2 Targeting to Multivesicular Bodies*. Int. J. Mol. Sci. 2019, *20* (5351), 1–16.

* Authors contributed equally

Paper III — **Nesverova, V.**; Wang, K.; Roche, J. V.; Gourdon, P.; Törnroth-Horsefield, S. *Single particle cryo-EM structure of a transient complex involved in aquaporin 2 trafficking*. Manuscript

Paper IV — **Nesverova, V.**; Järvå, M.; Kryh Öberg, F.; Törnroth-Horsefield, S. *Characterization of the interaction between aquaporin 5 and prolactin-inducible protein.* Manuscript

Paper V — Stefan,K.; Roche, J. V.; Missel, J. W.; Hagströmer, C. J.; **Nesverova, V.**; Gourdon, P.; Törnroth-Horsefield, S.: *The role of phosphorylation in calmodulin-mediated gating of human AQP0.* Manuscript

Publications not included in this thesis

Review — **Nesverova, V.**; Törnroth-Horsefield, S. *Phosphorylation-Dependent Regulation of Mammalian Aquaporins.* Cells 2019, *8* (82).

Contributions

Paper I — I performed the mass spectrometry experiments, analysed the data and prepared related tables. I contributed to manuscript writing.

Paper II — I created all AQP2 mutants, expressed and purified them and performed the binding studies with them. I planned, performed and analysed the stoichiometry experiments. I analysed all binding data and prepared related figures. I participated in interpretation of the result, writing the manuscript and figure-making.

Paper III — I expressed and purified both proteins and prepared the nanodiscs. I wrote the first draft of the manuscript and made most of the figures. I contributed to experiment planning and data interpretation.

Paper IV — I planned and performed all experiments and data analysis. I interpreted the results, wrote the first draft of the manuscript and made all figures.

Paper V — I performed the mass spectrometry experiments, analysed the data, prepared a related figure and contributed to manuscript writing.

Abbreviations

AOX1	Alcohol oxidase 1
AQP	Aquaporin
CaM	Calmodulin
cAMP	Cyclic adenosine monophosphate
CD	Circular dichroism
CD4	Cluster of differentiation 4
CHMP	Charged multivesicular body protein
CMC	Critical micellar concentration
Cryo-EM	Cryogenic electron microscopy
DED	Direct electron detector
EM	Electron microscopy
EP-GP	Extra-parotid glycoprotein
ESCRT	Endosomal sorting complex required for transport
FL	Full length
FSC	Fourier shell correlation
GCDFP-15	Gross cystic disease fluid protein 15
GOI	Gene of interest
IR	Infrared
LIP5	Lysosomal trafficking regulator-interacting protein 5
LMNG	Lauryl maltose neopentyl glycol
MALDI	Matrix-assisted laser desorption/ionization
MIM	MIT-interacting motif
MIT domain	Microtubule-interacting and trafficking domain

MSP	Membrane scaffold protein
MST	Microscale thermophoresis
MS/MS	Tandem mass spectrometry
MVB	Multivesicular body
ND	N-terminal domain
NDI	Nephrogenic diabetes insipidus
Ni-NTA	Nickel bound to nitrilotriacetic acid
NS EM	Negative stain electron microscopy
PAGE	Polyacrylamide electrophoresis
PCR	Polymerase chain reaction
PDB	Protein databank
PKA	Protein kinase A
PTM	Post-translational modification
SABS	Secretory actin-binding protein
SDS	Sodium dodecyl sulfate
SEC	Size exclusion chromatography
SS	Sjögren's syndrome
TEV	Tobacco etch virus
WT	Wild type

Scope of this thesis

Ahead in this thesis lie three stories of three aquaporins. I will introduce the curious reader to proteins in general and to aquaporins in particular. Then I will summarize the current wealth of knowledge about function and regulation of AQP2 in the kidney, AQP5 in the lacrimal and salivary glands and AQP0 in the eye lens. All of my practical research was done *in vitro* but in the background section you will hopefully receive the big picture of these three systems. After that I will summarize my findings from the five papers which are included at the end of this book. Even though the five papers have clear conclusions, these three stories are still very open-ended and the ends will be described in the Discussion chapter.

The aim of this thesis is to increase our understanding of how post-translational modifications and protein-protein interactions affect or regulate the function of aquaporins. This is a classic example of the structure-function relationship where the structure determines the details of the function. My postgraduate projects were all structure-focused and my attention was often on producing protein for crystallization for further structural determination by X-ray crystallography. During my time as a PhD student I have tried to crystallize various proteins, their mutants and I even tried to co-crystallize some of the proteins in complexes. Sometimes, I succeeded and obtained crystals but those were never good enough to produce diffraction that would help us obtain any new knowledge about the protein's structure. And as it often is in structural biology of membrane proteins, what was originally a side project became therefore my main project. I am grateful for that because apart from learning to accept failure, it also allowed me to learn a large variety of different techniques used for studying proteins, as you can read in the Methodology section. I do not want to spoil your reading experience but we did at the very end of my time as a PhD student shed some light on the structure of one of the complexes. But more on that later.

Proteins

Let us have a look at the composition of an average cell of human body. It is a well-known fact that water comprises two thirds of the mass of this cell and forms therefore the main component. In second place we will find proteins, responsible for 20 % of the mass. This is why proteins are often referred to as the "building material" of human body. But apart from creating the structures and shapes of our bodies, proteins have many other functions fundamental for life. Among proteins we can find hormones and other signalling molecules, receptors, the DNA replication apparatus, enzymes of the digestive system and molecules transporting other molecules to place where they are needed.

The word *protein* was for the first time used in a correspondence of a Swedish scientist Jöns Jacob Berzelius on the turn of the 19th century, deriving it from the Greek word *proteios*, meaning primary. He described proteins as "*la substance primitive ou principale de la nutrition animale que les plantes préparent pour les herbivores et que ceux-ci fournissent ensuite aux carnassiers*"- A primitive or principal substance of the animal nutrition which plants produce for the herbivores and which these then supply to carnivores [1].

Composed of amino acids bound in a linear strand, these strands often fold or bundle up to create the final but still somewhat flexible conformation. The three-dimensional structure is an absolutely critical property of each protein as it determines the function of the protein which is often carried out or regulated by interactions with other molecules. This structure-function relationship is what we have studied in this thesis, focusing on a particular type of proteins called aquaporins.

Water transport across the cell membrane

Each cell of our body is surrounded by a thin barrier composed of lipids and proteins, called the plasma membrane. This membrane protects the cell from the conditions and the substances outside of the cell. It selectively allows certain molecules to pass in an out of the cell according to the specific needs which are communicated by signalling proteins. Some molecules and gasses can cross the membrane by a simple diffusion in the lipid component [2]. Most molecules cannot cross the membrane directly and cells have therefore developed specialized protein channels and transporters. These are embedded in the phospholipid bilayer and either actively or passively transport molecules between the cytoplasm and the extracellular space or between the cytoplasm and the inside of various organelles. Membrane proteins are some of the most important drug targets for treatment of diseases, however they are notoriously difficult to study.

As I mentioned in the previous chapter water is the main component of our cells. It serves as a solvent for salts, some proteins, polysaccharides and DNA and the polar property of water is what drives protein folding and cell membrane formation in the first place. The amount of water on the cellular and organism level needs to be tightly and rapidly regulated to ensure appropriate salt concentrations and ionic gradients for energy generation. The specialized channels that allow water to pass across the cell membrane are called aquaporins.

Aquaporins

Present in all kingdoms of life, in every cell of human body, aquaporins (AQPs) are ubiquitous to life. They are passive transporters, letting water pass along the osmotic gradient – from the compartment of diluted electrolytes to the compartment with higher electrolyte concentration in order to maintain the integrity of the cell. Depending on the tissue and the type of membrane we can distinguish 13 isoforms of aquaporins in human. Interestingly, some aquaporins are also able to transport other small solutes while others are strictly water-specific. Those that transport only

water (orthodox aquaporins) are AQP0, AQP1, AQP2, AQP4 and AQP5 and the specificity is determined by the morphology of the pore itself. Aquaglyceroporins, a second type of aquaporins, can transport glycerol but often also urea and ammonia. AQP3 and AQP6-AQP10 belong to this group. Two aquaporins (AQP11, AQP12) of the human set are located solely subcellularly, in the membranes between the cytoplasm and various organelles. The permeability of these so called superaquaporins is not yet well established [3].

Aquaporins are involved whenever secretion is needed, participating in production of urine, sweat, saliva, tears and hydration of skin. Dysfunctional aquaporins have been linked to various diseases such as brain oedema, epilepsy, cancer and obesity either by mutations in the protein or by development of antibodies against a specific aquaporin [4].

Structural features

It has now been 20 years since the first structure of an aquaporin at atomic resolution was published, the one of AQP1 purified from red blood cells [5]. Since this breakthrough, the RCSB Protein Databank has registered more than 50 structures of aquaporins from many different organisms and new structures are being added every year. The similarities among these models are striking. Every aquaporin assembles as a homotetramer where each water pore functions individually (Figure 1). The pore is created by six transmembrane helices and a seventh pseudo-transmembrane helix created by two loops dipping into the membrane from opposite sides. An aquaporin monomer is typically 27-30 kDa in size.

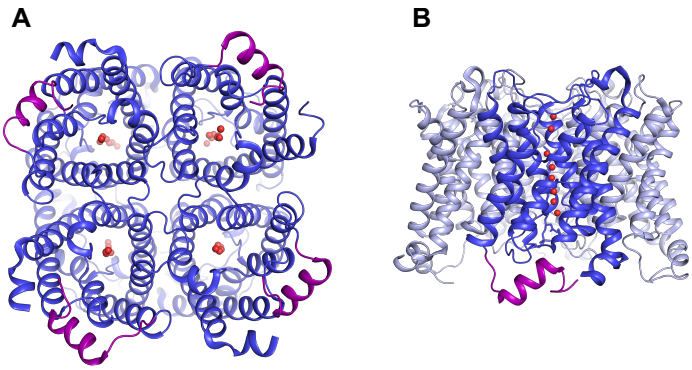

Figure 1. The common structure of aquaporins shown by the crystal structure of human AQP5 (PDB code 3D9S). **A.** View from the cytoplasmic side, revealing the homotetrameric arrangement with four pores containing single files of water molecules (red spheres). **B.** Side view with the frontmost monomer colored in darker blue. The conserved C-terminal helix is highlighted in purple.

The amino acid residues lining the inside of the pore determine the specificity of the channel. In water-specific AQPs, the pore is just narrow enough for a single file of water molecules to *queue* their way through (Figure 1B). Two copies of the signature motif NPA (asparagine, proline, alanine) constrains the orientation of passing water molecules, creating an electrostatic barrier for proton (and other cation) exclusion. The narrowest part of the channel is the ar/R selectivity filter (aromatic residue, arginine) located near the extracellular end which acts as a constriction region, preventing the passage of larger molecules but also contributing to proton exclusion [6]. This region is typically slightly wider in aquaglyceroporins to allow for transport of larger solutes [7].

Both the N- and C-termini are always located in the cytoplasm, however their length and amino acid composition differ greatly between the isoforms. While not being part of the channel itself, the termini serve an important role in the regulation of water transport through the channel and it is generally on the termini that regulatory proteins bind [8]. Post-translational modifications such as phosphorylation and ubiquitination of the residues of the termini (and sometimes also of the cytoplasmic loops) are also important for regulation and often alter the affinity for binding of these regulatory proteins [9].

In mammalian AQPs, the proximal part of the C-terminus often assumes a secondary structure of a short alpha-helix (Figure 1B). In AQP2 this helix assumes an unusual flexibility in its relative orientation within the tetramer. This is caused by two consecutive prolines (Pro 225 and 226) which function as a hinge [10]. The C-terminal helix is a known binding site for interacting regulatory proteins in AQP2 and AQP0 [8], which will be described in great detail further on in this thesis.

Aquaporin regulation

To ensure a tight control over the inner environment of every cell, the amount of water passing in or out needs to be regulated. Three distinct mechanisms of regulation exist, the slowest of which is the regulation of the transcription and translation of the gene coding for the protein. For rapid control, eukaryotic organisms have developed post-translational means of regulation on the single molecule level – either the channel can open and close (gating) or the protein can be shuffled between the plasma membrane and storage vesicles (trafficking) [7] (Figure 2).

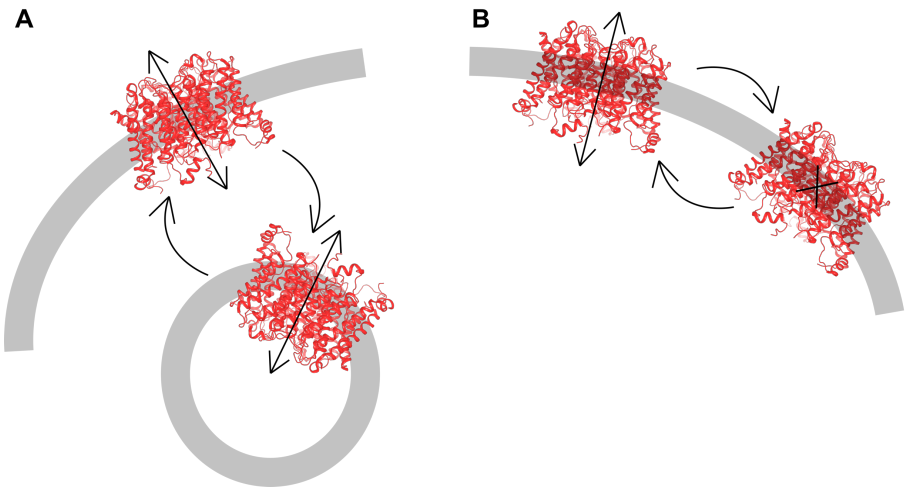

Figure 2. Post-translational regulation of the water permeability of aquaporins happens by two distinct mechanisms. **A.** Trafficking between the storage vesicles and the plasma membrane; **B.** Opening and closing the pore by gating.

Gating

The opening or closure of the aquaporin water channel happens upon a trigger, often mediated by a post-translational modification. This regulatory mechanism is very common in plant aquaporins because plants need to quickly react to fluctuations of water supply during the times of draught or flooding. Here the gating happens through an intracellular loop D which changes conformation to effectively occlude the pore [11]. Some human aquaporins have also been suggested to be gated, although here the mechanism is less common.

The most studied gated human aquaporin is AQP0, abundant in the eye lens, where it maintains lens transparency and facilitates microcirculation [12]. The gating of AQP0 is dependent on intracellular Ca^{2+} concentrations and binding of the regulatory protein calmodulin, where the binding of calmodulin in the Ca^{2+}-bound form causes AQP0 closure [13]. This is further regulated by phosphorylation of AQP0 C-terminus [14]. Gating of the water pore has been also suggested for AQP4 [15], AQP5 [16,17] and AQP10 [18].

Trafficking

Another way of regulating the amount of water passing through the membrane is by affecting the abundance of aquaporin molecules present. Shuttling the protein between the plasma membrane and the storage vesicles is a neat mechanism, though

regulated by a number of stimuli [19]. The most common triggers are hormones (vasopressin, adrenalin, histamine), other small molecules (acetylcholine, glutamate) and hyper- or hypotonicity [19]. The triggers are then effected by binding of regulatory proteins which in turn initiates the trafficking of the aquaporins to their destination [8]. For example, the endo- or exocytosis of the aquaporin-containing vesicles is guided by interaction with microtubules [20]. The binding of regulatory proteins is itself often regulated by post-translational modifications, specifically by phosphorylation [9].

Aquaporins studied in this thesis

In this thesis I have studied three isoforms of human aquaporins, all of them orthodox aquaporins, and how they interact with and are regulated by three respective interaction partners. AQP0, AQP2 and AQP5 share between 53 % and 66 % sequence identity between each other. However, the C-terminus where all of the regulatory proteins bind is on average 13 % less identical [21]. The uniqueness of the C-termini contributes to the specificity of the binding and to the underlying regulatory mechanism.

As mentioned above, the water transport through AQP0 is regulated by gating, which happens upon binding of calmodulin. Both AQP2 and AQP5 are regulated by trafficking where AQP2 responds strongly to vasopressin as a trigger. The trafficking of AQP2 is determined by a phosphorylation *code*, each of the four known phosphorylation sites deciding the sub-cellular localization of the protein. AQP5 trafficking responds to extracellular hypotonicity, the activity of protein kinase A and phosphorylation [22].

Story 1: Water reabsorption in the kidney collecting duct

In the previous chapter I have introduced aquaporins as channels crucial for transport of water in and out of the cell. This and the next two chapters will bring the protein into a living context of three systems in the human body. We will dive into the urinary system to see how aquaporins help us regulate the urine volume. We will unravel how aquaporins take care of tear and saliva production. Later, we will study the visual system and how aquaporins maintain the water balance in the eye.

In the kidneys eight of the thirteen human aquaporin isoforms were found to be expressed. AQP1, AQP4, AQP7 and AQP11 were identified in the proximal part of the tubules while in the collecting duct AQP2, AQP3, AQP4 and AQP6 are present [23]. In the glomerulus blood is filtered with a filtration rate of more than 100 ml/min. This primary urine needs to be concentrated and water reabsorbed, which to a large constitutive extent happens in the proximal tubule. The collecting duct is responsible for hormone-regulated reabsorption and here the final volume of urine is determined [24].

In the principal cells lining the collecting duct, AQP2 mediates the flux of water from the duct into the cell through the apical membrane, while AQP3 and AQP4 allow the water to leave the cell through the basolateral membrane [25] (Figure 3). Certain single amino acid mutations in AQP2 are known to lead to nephrogenic diabetes insipidus (NDI), a genetic disorder characterized by large urine volumes and dehydration. This is often caused by misfolding of the mutated protein, its inability to oligomerize or interference with the trafficking regulation mechanism [26]. NDI can also be acquired, a condition that is characterized by decreased AQP2 expression levels. This can be a side effect of drug treatments and is seen as part of various conditions like nocturnal enuresis and acute or chronic renal failure [25]. It is therefore important to unravel the cellular and molecular details of how AQP2 is regulated in order to design appropriate treatments.

AQP2 responds to hydration levels

When the osmolarity of the extracellular fluid of the body is too high (dehydration) the hormone vasopressin is released from the pituitary gland. Vasopressin reaches the kidneys quickly through the blood stream and binds to the vasopressin V_2- receptor in the basolateral membrane of principal cells. This triggers an intracellular signalling cascade resulting in increased concentration of cyclic adenosine-3',5'-cyclic monophosphate (cAMP), leading to activation of protein kinase A (PKA). Activated PKA reaches the AQP2 in storage vesicles and phosphorylates serine 256. This is a key event for the AQP2 translocation to the apical membrane, therefore increasing the apical membrane water permeability and allowing rapid urine concentration to happen [25,27] (Figure 3). As a result, the optimal osmolarity of the interstitial fluid in the body is maintained.

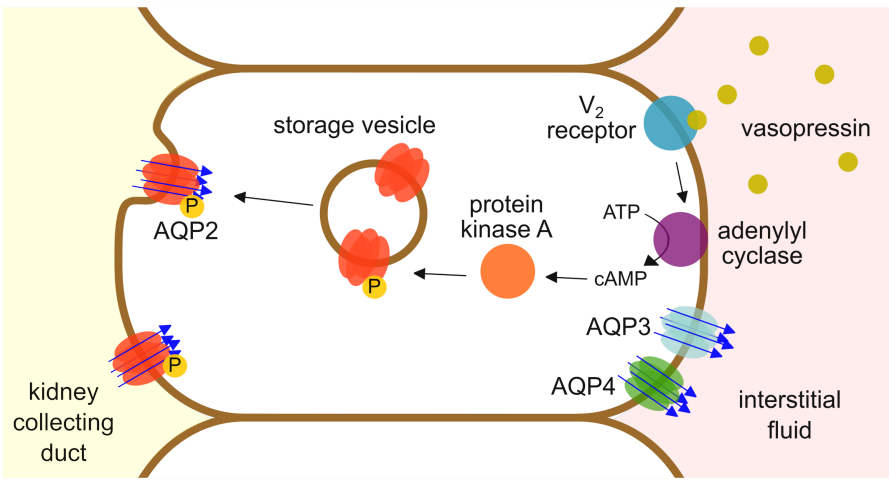

Figure 3. Schematic representation of the vasopressin-dependent exocytosis of AQP2 in a principal cell of the kidney collecting duct. Upon binding of vasopressin to the V_2-receptor at the basolateral membrane the increase in cAMP concentration results in activation of protein kinase A. This enzyme phosphorylates AQP2 which causes its translocation to the apical membrane. Water can then enter the cell from the kidney collecting duct and leave the cell through AQP3 and AQP4 on the basolateral membrane.

The optimal hydration level has been restored and the level of vasopressin drops. The removal of vasopressin from its receptor (or the activation of protein kinase C) results in ubiquitination of AQP2 on lysine 270. AQP2 is then internalized and targeted for further sorting by the endosomal sorting system. The water uptake from urine has decreased and AQP2 may be degraded in lysosome, excreted into the urine in form of exosomes or deubiquitinated and stored in vesicles for another round of vasopressin stimulation [28].

Phosphorylation controls the sub-cellular localization of AQP2

Phosphorylation is one of the most common protein regulation mechanisms. This reversible post-translational modification can induce a variety of effects such as changing the protein conformation or promote/inhibit protein-protein interactions. The addition of a phosphoryl group onto a serine, threonine or tyrosine is performed by a group of enzymes called kinases. Contrarily, phosphatases are responsible for selectively removing the phosphoryl groups. These enzymes often need to be activated in order to gain enzymatic activity which presents an additional layer of complexity in protein function regulation [9].

For AQP2, phosphorylation plays a major role in regulation of urine volume by affecting the preferred sub-cellar localization of the protein. Four phosphorylation sites were identified *in vivo* in human AQP2: S256, S261, S264 and T269, all of them located on the distal C-terminus [29,30]. Phosphorylation or dephosphorylation of these residues affects the affinity of AQP2 to its interaction partners, which in turn alters the protein's sub-cellular localization. A fine interplay between phosphorylation and dephosphorylation is the key for effective regulation [9]. As described in the previous subchapter, phosphorylation of S256 is necessary for exocytosis of AQP2 [29]. Once in the apical membrane, further phosphorylation on T269 stabilizes the protein and increases AQP2 retention time [31] (Figure 4A). S261 is mainly phosphorylated when AQP2 is stored in intracellular vesicles and dephosphorylation of this residue coincides with vasopressin stimulation [32]. Phosphorylation of S264 was detected in plasma membrane and early endosomes but not in lysosomes. This phosphorylation therefore presumably protects AQP2 from being targeted for lysosomal degradation and has been suggested to be involved in secretion of AQP2 in exosomes [33] (Figure 4B).

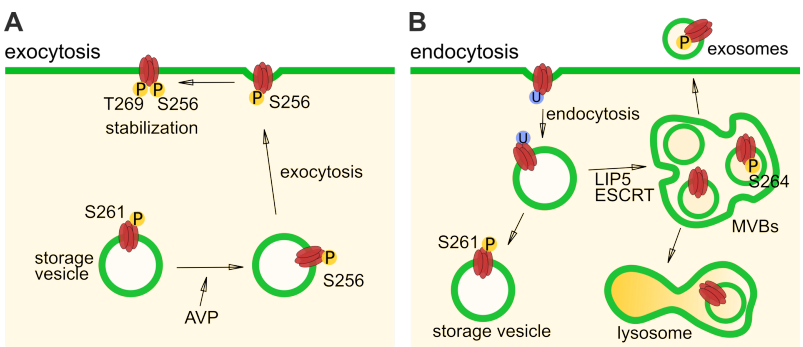

Figure 4. Schematic representation of the different subcellular localizations of AQP2 in different phosphorylation states. **A.** during exocytosis; **B.** during endocytosis. Figure adapted from [9].

Aquaporin sorting to multivesicular bodies

When AQP2 is no longer needed in the apical membrane it is ubiquitinated on lysine 270 [28] by E3 ligases [34]. This is a signal for its endocytosis (Figure 4B). AQP2 can then be deubiquitinated, phosphorylated at S261 and stored until needed again. Upon prolonged ubiquitination the protein will be targeted to multivesicular bodies (MVBs) by the endosomal sorting machinery (Figure 5). MVB is a late endosome containing many small inner vesicles which are created by inwards budding of the endosomal membrane. These inner vesicles contain membrane proteins which the cell no longer needs or which are misfolded. This way AQP2 (or other cargo proteins) can by degraded by fusion of the MVB with lysosome, alternatively the inner vesicles can be released outside of the cell as exosomes when the MVB fuses with the plasma membrane [28].

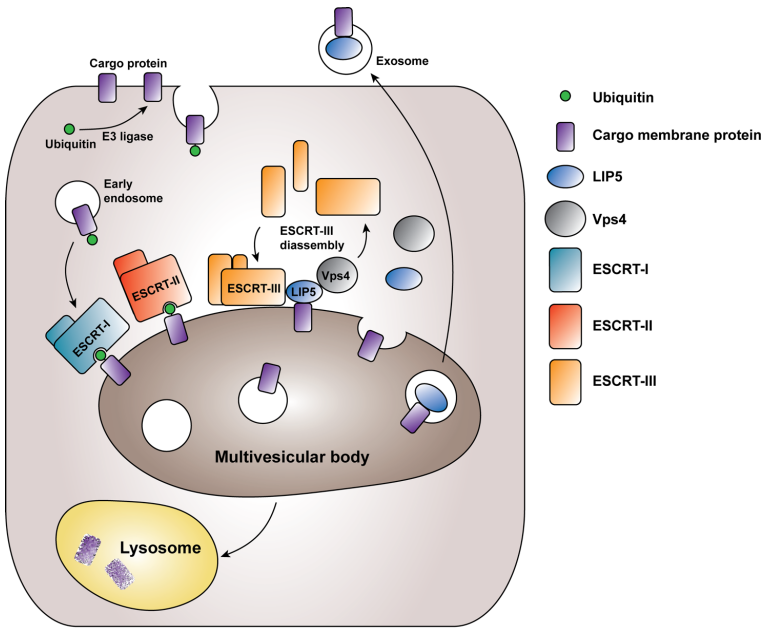

Figure 5. Overview of the endosomal sorting machinery. Ubiquitinated membrane proteins are recognized by ESCRT-I and ESCRT-II after which the concerted actions of ESCRT-III, Vps4 and LIP5 result in their insertion into inner vesicles of multivesicular bodies. Figure reproduced from [35].

The formation of the inner vesicles and therefore of the MVBs is governed by the sequential binding of four highly conserved complexes called Endosomal Sorting Complexes Required for Transport (ESCRT). These recognize ubiquitinated membrane proteins and cause membrane bending and budding. In the final step the transient ESCRT-III complex forms a membrane bound fibre, assisting the protein

deubiquitinating and membrane scission. The ESCRT-III complex is disassembled and the membrane vesicle formation finished when the Vps4 ATPase double hexameric ring binds to it [36]. However, this will only happen if Vps4 is activated by binding a soluble Lysosomal Trafficking Regulator-Interacting Protein 5 (LIP5) [37].

LIP5 coordinates the inner vesicle formation

Apart from being the activator of the Vps4, LIP5 was found to bind to different parts of the ESCRT-III heteropolymer fibres [38–40] as well as to AQP2 [41]. This suggests that LIP5 plays a role in coordinating the function of these three components (Figure 5).

LIP5 is a 34 kDa protein with two distinct domains which are separated by a long flexible linker [40]. The N-terminal domain consists of 6 helices organized into two bundles (Figure 6A) where each bundle comprises one microtubule-interacting and trafficking (MIT) domain. Here the ESCRT-III components can bind through their MIT-interacting motifs (MIMs) [40]. The C-terminal domain of LIP5 forms a helical hairpin which upon dimerization binds Vps4 [37] (Figure 6B).

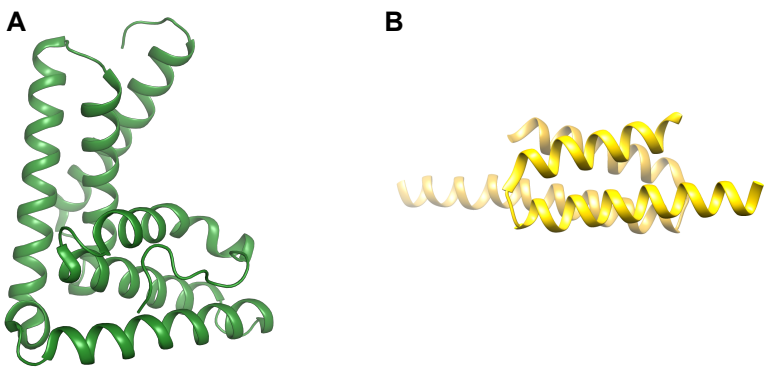

Figure 6. **A.** Structure of LIP5 N-terminal domain (PDB code 4TXQ) consisting of two bundles of three helices making up the two MIT domains; **B.** Structure of dimerized C-terminal domain of LIP5 yeast homologue Vta1 (PDB code 2RKL).

The AQP2-LIP5 interaction was first described by van Balkom et al [41] where LIP5 was found to interact with the C-terminus of AQP2, used as a bait in a yeast two hybrid assay. This was also the first time that LIP5 was reported to bind directly to the membrane protein cargo. This might be a general mechanism as LIP5 was also found to bind an EGF receptor [41]. The region between residues 230 and 243 of

AQP2 was suggested to be the binding site [41]. Interestingly, the sequence contains a MIM motif LXXRLXXL(K/R), also present on different proteins from the ESCRT-III complex [42]. We hypothesised that it is this motif that binds to the MIT motif on LIP5 and we have tested this in Paper II using site-specific mutagenesis.

As described earlier the specific phosphorylation *code* affects the cellular localization of AQP2 by altering the affinities towards interacting partners involved in trafficking. Understanding the nitty gritty details of these processes help us form a complete picture of how the hydration of our bodies is maintained by the kidneys. The effect of the AQP2 phosphorylation on the binding affinity for LIP5 was studied in Paper I. Moreover, the binding interface of the AQP2-LIP5 interaction was the subject of our investigation in Paper II. Finally, in Paper III our cryo-EM structure of the AQP2-LIP5 complex provides insights into the binding mode.

Story 2: Water secretion by lacrimal and salivary glands

Tears, saliva, sweat and pulmonary fluid are all secreted through AQP5 [43], which is present at the luminal membrane of cells lining the secretory glands. These secretions are crucial in order to prevent infection of mucous surfaces and to facilitate the proper function of vision, swallowing, digestion and breathing.

Similarly to AQP2, also the AQP5 function is also tightly regulated by trafficking. Both the shuttling of the protein between the apical membrane and the intracellular vesicles and the transcription rate are regulated on many levels, for example by intracellular cAMP concentrations, protein kinase A (PKA) activity, phosphorylation of Ser 156 and hypotonic conditions [22]. Contrarily from AQP2, AQP5 trafficking is currently far less understood. A few suggestions of AQP5 gating exist but this mechanism of regulation has not been conclusively proven for this isoform [16,17].

Sjögren's syndrome

The abnormal distribution of AQP5 in the secretory glands leads to dryness of mucous surfaces and a condition called Sjögren's syndrome (SS). AQP5 was found to be present primarily in the basal membranes of salivary glands [44] and in the cytoplasm of lacrimal glands [45] of SS patients, compared to its apical membrane presence in healthy volunteers and patients with non-SS dry eye disorders. Autoantibodies against the M3 muscarinic receptor were shown to decrease trafficking of GFP-fused AQP5 in human salivary gland cells. These antibodies are present in the plasma of SS patients [46]. Some studies suggest that even AQP4 [47] and AQP1 [48] trafficking might be dysregulated in SS.

The characteristic symptoms of SS are dry mouth and dry eyes, causing problems in everyday life. Most patients are post-menopausal women but other than the hormonal influence the SS development seems to be also genetically conditioned [49]. The disease is characterized by autoimmune lymphocyte infiltration of the

lacrimal and salivary glands and recently the presence of anti-AQP5 antibodies was discovered which is a promising potential biomarker for SS [50].

PIP ensures correct regulation of AQP5

Prolactin-inducible protein (PIP) was identified as an interaction partner for AQP5 with implications for SS [51]. In this study, a peptide corresponding to AQP5 C-terminus was immobilized on a column and mouse lacrimal gland homogenate was passed through. PIP was found to bind to AQP5 in samples from healthy mice but not from mice models for SS. Immunohistochemistry with anti-AQP5 and anti-PIP antibodies confirmed similar cellular localization of both proteins at the apical membrane of lacrimal gland cells of healthy mice. A treatment with antisense PIP oligonucleotides in order to decrease the PIP expression resulted in altered AQP5 cellular distribution. The authors therefore concluded that the binding of PIP is needed for correct trafficking of AQP5 [51]. To the best of my knowledge there are no other published studies investigating this interaction.

The absence of PIP seems to be one of the hallmarks of SS. In SS rabbit models PIP was found to be downregulated in the tears, compared to healthy rabbits [52]. The same trend was also observed in human saliva and the PIP mRNA was lowered in salivary glands of SS patients pointing towards decreased PIP production during the condition [53].

PIP is a small protein which was discovered independently in many different tissues and it was therefore given several names. As prolactin-inducible protein it was first discovered in human breast cancer cells upon prolactin stimulation [54]. As gross cystic disease fluid protein 15 (GCDFP-15) it was isolated from the breast cyst fluid [55] and from human seminal plasma it was described as secretory actin-binding protein (SABS) [56]. In saliva it was named extra-parotid glycoprotein (EP-GP) [57]. After discovering this CD4-binding protein in human seminal plasma and naming it glycoprotein gp17, the researchers has realized that all of these were in fact the same protein [58].

The function of PIP is extremely wide. It is for example involved in viral infection and tumour progression, in seminal plasma it has a role in fertilization and in saliva it modulates bacterial colonization of the enamel surface [59]. Structurally, PIP consists of a sandwich arrangement of two β-sheets made of seven β-strands (Figure 7). A glycosylation site is present on Asn 77, glycosylation of which seems to be important for protein stability since in the PIP crystal structure the glycan was involved in hydrogen bonds toward two neighbouring loops [60] (Figure 7). PIP is a secreted protein and the sequence therefore contains a secretion signal sequence

which is cleaved off during protein maturation. The mature unglycosylated protein has a predicted size of 13.5 kDa. Thanks to a different glycosylation content varying protein sizes are reported in PIP from different tissues or secretions [56,58,61].

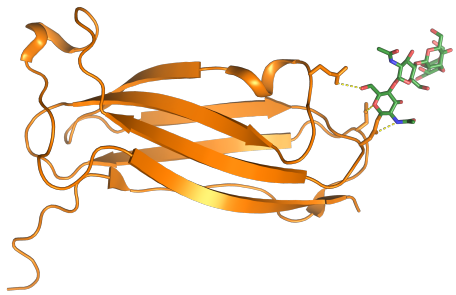

Figure 7. Structure of PIP (PDB code 3ES6) consisting of two β-sheets created by seven β-strands. In the crystal structure asparagine 77 is glycosylated by four glycan residues (green), connecting the three neighbouring loops by hydrogen bonds.

It is fascinating that PIP was found to bind such a large number of targets. Apart from AQP5 the interactome also contains CD4 receptor [62], actin [56], human serum albumin [63], immunoglobulin G [64], zinc-α-glycoprotein [65] and many more. In Paper IV we have characterized the binding between AQP5 and PIP *in vitro*, providing the first details into the AQP5-PIP complexation. Such knowledge could help understand the role of PIP in AQP5 trafficking and development of SS.

Story 3: Water balance in the eye lens

AQP0 maintains lens transparency

For a proper function of the eye the individual ocular components need to be hydrated. Moreover, the intraocular pressure and the lens transparency need to be maintained. The movement of water in the eye also promotes effective removal of metabolic products and rapid changes in water content in various parts of the eye facilitate the pupil constriction and dilatation. Aquaporins play an important role in this and are also responsible for tear secretion. Five human aquaporins are known to maintain the healthy ocular function – AQP0, AQP1, AQP3, AQP4 and AQP5 [12].

In this chapter I will focus solely on AQP0 and its role in the eye. In lens fibre cells AQP0 is the main protein component of the plasma membrane [66], ensuring lens transparency. Humans with mutant AQP0 develop hereditary cataract [67]. Here, AQP0 does not have its main function as a water channel but rather as an adhesive protein, creating thin junctions between two adjacent cells by two AQP0 tetramers interacting with each other. This way AQP0 controls the spacing between the fibre cells even as the lens changes its shape during focusing, making sure that the spacing is smaller than the wavelength of visible light and therefore the lens appears transparent. Creation of the arrays of AQP0 pairs is promoted by a proteolytic cleavage of the C-terminus during eye maturation [68]. This ability of AQP0 to form arrays was exploited for molecular structure determination using 2D crystals in electron crystallography [69].

Calmodulin regulates AQP0 gating

The permeability of AQP0 is tightly regulated to ensure optimal hydration of the lens. Three distinct mechanisms of regulation exist. As described above, C-terminal cleavage leads to formation of junctions as well as pore closure through the shift of the loop A, which also mediates the contact within the junction [70]. For intact full-length AQP0 the water permeability is dynamically regulated by two additional mechanisms. The change in pH has an effect on the permeability of AQP0 in

Xenopus oocytes where lowering the pH causes increase in the permeability. This effect is likely governed by the His 40, which is unique for AQP0 [71]. Additionally the binding of a small regulatory protein calmodulin (CaM) upon presence of high intracellular Ca^{2+} concentrations closes the pore [13].

Calmodulin is a 16.8 kDa Ca^{2+}-sensing protein which upon binding of four molecules of calcium changes its conformation and binds to an enormously diverse variety of other proteins. It consists of two bundles of three short helices, each containing a pair of EF-hands (Figure 8A). These two bundles are connected by another longer and flexible helix. Through this binding CaM translates the intracellular Ca^{2+} levels onto many regulatory signalling pathways [72].

On AQP0 the CaM-binding site was found to be the short C-terminal helix [73] and CaM was suggested to bind two copies of these helices from the neighbouring monomers. This binding mode is often described as non-canonical as CaM typically binds only one α-helix [74]. The resulting stoichiometry of two molecules of CaM binding one AQP0 tetramer was further endorsed by a pseudo-atomic negative stain EM model of the complex [75] (Figure 8B). This model, with the help of molecular dynamics simulations, suggests that the binding of CaM does not occlude the pore, instead the complexation allosterically stabilizes AQP0 in a closed conformation at a second constriction site (CSII) located near the cytoplasmic end of the pore. It is mainly Tyr 149 that is believed to flip to narrow the pore width down to 1.5 Å which would occlude the channel [76].

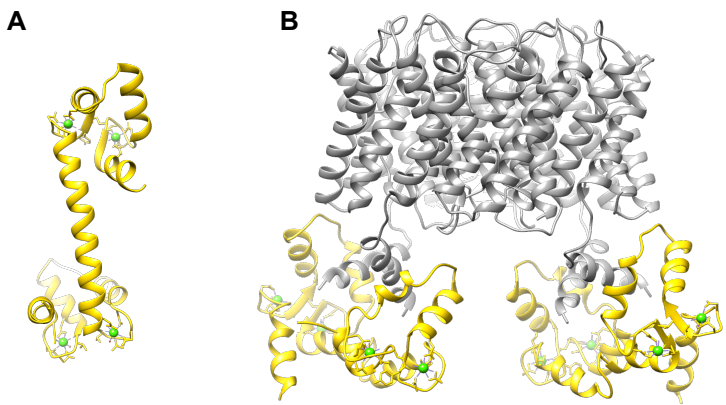

Figure 8. A. Structure of calmodulin (CaM) in the calcium bound form (PDB code 1CLL). Four EF-hands bind four atoms of calcium (green spheres); **B.** Structural model of the AQP0-CaM complex (PDB code 3J41). Two molecules of CaM bind to each AQP0 tetramer, with each CaM binding two helices from neighbouring AQP0 monomers.

Phosphorylation of AQP0

The addition of phosphoryl group onto the C-terminus of AQP0 plays a role in the gating by affecting the binding affinity towards CaM. There are three phosphorylation sites present in AQP0: Ser 229, Ser 231 and Ser 235 [9], all part of the conserved cytoplasmic helix. When either S231, S235 or both were phosphorylated, the binding of CaM was severely impaired, this was however only tested with short peptides corresponding to the AQP0 C-terminus [77]. In *Xenopus* oocytes, the water permeability of the phosphomimicking mutant S235D still retained its calcium sensitivity, suggesting that AQP0 phosphorylated at S235 might still be able to bind CaM. Both S229D and S231D lost its calcium sensitivity and the water permeability was increased [14]. Interestingly, phosphorylation of the S235 by protein kinase C also affects AQP0 sub-cellular localization and seems to be crucial for translocation of the protein to plasma membrane after synthesis [78].

In Paper V we have investigated the effect of phosphomimicking AQP2 mutations on the binding affinity to CaM using purified full-length proteins. Moreover, we have examined the calcium and CaM effect on the water transport capabilities of these mutants in proteoliposomes.

Methodology

From gene of interest to a protein sample

Cloning and mutagenesis

In the 19th century proteins were very difficult to obtain in the large quantities needed for biochemical studies and therefore only proteins naturally abundant (like insulin obtained from slaughterhouses and albumin from egg white) were being characterized. Revolution came with the development of homologous recombination and gene transfer which required us to first understand our genetic code and to learn how DNA can be manipulated. Nowadays, these technologies allow us to study even very weakly abundant proteins.

The standard cloning strategy which we use in our laboratory includes the amplification of gene of interest (GOI) during PCR using specifically designed set of primers. The use of restriction enzymes allows us to create compatible ends by which a piece of DNA can be connected to another using a ligase. By copying and pasting sequences new constructs are created. The choice of vector into which a GOI is pasted depends on the selected expression host, selected promotor for induction of expression and desired tags.

In Papers I, II and V we studied the effect of single amino acid mutations on various properties of the proteins. To generate site-directed mutations in the sequence of DNA we used the megaprimer approach where a megaprimer is first generated in PCR using one universal primer and one primer introducing the mutation. This megaprimer was then used for a second round of PCR to amplify the entire plasmid [79]. Using this method, the use of ligase can be avoided and the whole process of generating mutations is faster and more straight-forward.

Recombinant protein expression

A gene of interest cloned into a suitable vector is transformed into the host cell. Either bacteria, yeast or insect cells may be suitable for protein overexpression and isolation, depending on the particular protein of interest. For the expression of

mammalian membrane proteins eukaryotic organism are used with great advantage thanks to the more elaborate folding machinery and the ability to perform post-translational modifications [80].

In our laboratory, aquaporins have been successfully expressed in the yeast *Pichia pastoris* [81] with high enough yields to allow the structural determination of AQP2 [10], AQP5 [82] and spinach aquaporin SoPIP2;1[83]. *Pichia pastoris* is a methylotrophic yeast which means it can survive on methanol as a sole carbon source. This quality is successfully coupled with using the alcohol oxidase 1 (AOX1) promotor which is heavily induced in the presence of methanol, driving the recombinant protein expression. Moreover *P. pastoris* can be grown to very large densities, compared to another commonly used yeast *S. cerevisiae*, which increases the chance of high protein yields [84].

In practice, a pPICZ vector containing the sequence for an aquaporin is transformed into the *P. pastoris* strain x-33 by electroporation. The transformed clones are grown on Zeocin-selective plates where the higher the Zeocin resistance the more copies of the plasmid were incorporated and therefore higher protein expression levels are to be expected.

Small-scale expression screening using buffered complex media and methanol induction were used to check the expression levels of highly zeocin-resistant clones. The top expressing clone for each construct was then grown at a large scale in a 3L fermenter under tightly controlled conditions. Each batch of fermentation yielded 400-600 g of cells. We have used *Pichia pastoris* for expression of PIP as well, however, here the protein was secreted into the media thanks to the α-secretion signal present on the plasmid.

For the soluble protein LIP5 and its various constructs *E. coli* expression system was used under the control of lac operon. The protein was expressed for 4 hours at 30 °C in the standard LB-media.

Solubilization and purification

In order to be able to study a protein *in vitro* using the methods described in further subchapters, the protein of interest needs to be isolated from all the other thousands of proteins expressed by the host at the same time.

For purification of a membrane protein the membrane fraction of a cell needs to be isolated first. Various methods of cell lysis exist, in our laboratory we used the bead-beater to grind the cells with glass beads. Differential centrifugation separates the cell debris from the membranes which are then spun at higher speeds. Membranes can

then be washed with urea to remove weakly bound and interacting proteins, increasing the chance of successful purification.

After membrane isolation the membrane protein needs to be solubilized with the help of a suitable detergent in order to cover the hydrophobic parts of protein which are otherwise buried in the phospholipid membrane (Figure 9). The concentration of the detergent has to be above the critical micellar concentration (CMC) for the micelles to start forming and for the protein to be solubilized out of the membrane. Typically, a large excess of the detergent is added to maximize the solubilization efficiency, this however results in a formation of empty micelles (Figure 9C and D). The choice of detergent depends greatly on the planned downstream application and is a trade-off between chemical properties, stability, yield and size of micelle.

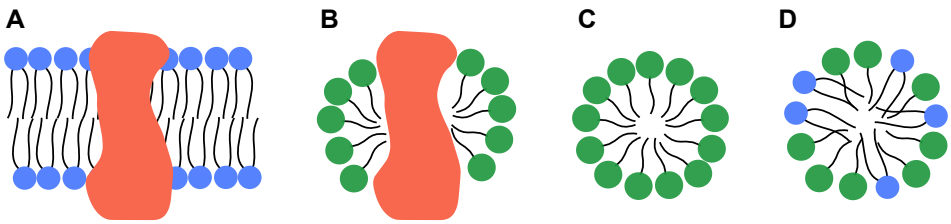

Figure 9. Solubilization of membrane proteins with detergent. **A.** An intergral membrane protein (orange), embedded into the cellular phospholipid bilayer (blue); **B.** Upon addition of detergent (green) at concentrations above the CMC, the detergent strips the protein off the membrane and covers the hydrophobic parts of it. Inevitably, empty detergent micelles (**C.**) and mixed phospholipid-detergent micelles (**D.**) also form.

The purification of soluble proteins is significantly simplified by the fact that no membrane preparation nor solubilization is necessary. These proteins can be purified directly from the supernatant of cell lysate.

Genetic engineering allows the addition of pieces of DNA to the construct which when translated results in tags commonly used for simplified protein detection and purification. In our case both AQP2 and LIP5 carried a poly-histidine tag (His-tag), though AQP2 had an uncleavable His-tag on the N-terminus while LIP5 construct contained the His-tag on the C-terminus, preceded by a tobacco etch virus (TEV) protease cleavage site and a spacer. We could therefore simply purify the proteins using affinity chromatography in a nickel column.

Size exclusion chromatography (SEC) serves as a purification step but also as a check for sample quality and homogeneity. Any significant protein aggregation will be detected during the run. When comparing batches, the same protein should always elute at the same retention volume and the elution peak should ideally be symmetrical and monodisperse.

Sample characterization

Mass spectrometry

The analysis of a mass spectrum of sample is a powerful method of answering the question: What protein are we dealing with? Typically, but not always, a protein sample (either a liquid sample or an excised piece of an SDS-PAGE gel) is digested with a protease like trypsin or chymotrypsin. The peptides are then ionized and the mass to charge ratio (m/z) based on the time-of-flight is measured. In tandem mass spectrometry (MS/MS) each detected peptide could be further isolated and fragmented. The resulting m/z of the individual amino-acids reveals the sequence of the peptide including possible post-translational modifications.

In my work I have used mass spectrometry to confirm the identity of the proteins of interest and to study what kind of contaminants there are in my sample (know your enemy approach). In Paper I we have used the method to study post-translational modifications, specifically to determine whether human AQP2 gets phosphorylated when expressed by *P. pastoris*. Human AQP0 is known to lose its C-terminus when maturating in the human eye lens [69]. We have used mass spectrometry in Paper V to verify that our recombinantly expressed AQP0 still contains the C-terminus which is the binding site for CaM. This was done on an undigested sample using the linear mode MALDI to detect the entire mass of the intact protein.

Phosphorylation detection

When studying the effect of phosphorylation on some other properties of the protein it is crucial to know the phosphorylation status of the protein. Apart from the already mentioned mass spectrometry, another way to detect phosphorylation is using phosphate monoester-detecting Phos-tag BTL-111 coupled with biotin, which is then detected by streptavidin-HRP during western blot [85]. We used this method in Paper I when we studied the effect of phosphorylation of AQP2 C-terminus on the interaction with LIP5. Specific phosphomimicking mutants of AQP2 were produced and residual phosphorylation was removed by treatment with alkaline phosphatase. We then used this Phos-tag to verify that the treatment was successful. In Paper V we used this method to verify that AQP0 is not phosphorylated when expressed in *P. pastoris*.

Circular dichroism

A standard way of assessing the secondary structure, the folding and the stability of proteins is circular dichroism (CD). This method utilizes the fact that proteins are very chiral molecules. The difference in absorbance between left and right circularly polarized light is referred to as ellipticity θ. The absorbance in the far UV region (190-240 nm) corresponds to the peptide bond which acts as chromophore when ordered into a secondary structure. Each secondary structure (alpha helix, beta sheet, random coil and even some less common structures) has its signature CD spectrum. The spectrum of a sample is then an average of all secondary structures present in the sample. Deconvolution of this spectrum is still very challenging but for purified proteins CD allows an estimation of a secondary structure content.

In order to study a thermal stability of a protein the sample is slowly heated and corresponding CD spectra are recorded. As the sample melts the protein is unfolding and therefore losing the light absorbing properties of the peptide bond in the secondary structure. The ellipticity at a specific wavelength in dependence on the temperature allows a construction of a melting curve and calculation of melting temperature. This way the effect of various buffer components, ligands and point mutations on the protein stability can be studied as we did in Paper I with phosphomimicking constructs of AQP2.

Assaying protein binding

Molecular recognition governs all biological processes in the cell. Complexes of two or more molecules are held together by hydrogen bonding, van der Waals, hydrophobic and ionic interactions. These interactions are rather weak and a mixture of interacting proteins is therefore at an equilibrium of unbound and bound states [86].

Two parameters describe molecular recognition: affinity and specificity. High affinity binding is often achieved by increased hydrophobic interactions between the proteins and this determines the stability of the complex. Specificity of the binding is critical for the function of the complexation and will depend on formation of hydrogen bonds. It refers to a relative strength of binding if comparing several interaction partners, where one protein would bind to a specific partner but not bind to others [87]. Although two proteins can have the same affinity for a third protein, the specificity might differ.

The affinity of a protein-protein interaction is characterized by the dissociation constant K_D. The dissociation constant is the equilibrium constant for the reaction between protein A and protein B:

$$A \cdot B \rightleftharpoons A + B$$

K_D is then defined:

$$K_D = \frac{[A][B]}{[A \cdot B]}$$

K_D is in its magnitude equal to [A] at which half of protein B is bound to protein A and half is unbound (fractional saturation is 0.5). Although the constant is a dimensionless number, because of this fact it is often considered as if it has molar units of concentration.

Binding assays probe the binding affinity by measuring the amount of protein A bound to the protein B at various concentrations of protein A. This measurement allows construction of a binding isotherm which is often shown in its logarithmic form (Figure 10). When saturation of the protein B with protein A is possible it is a sign of a well-defined specific binding site [86]. In the next subchapters I will describe the methods we have used to study the interactions between aquaporins and different regulatory proteins.

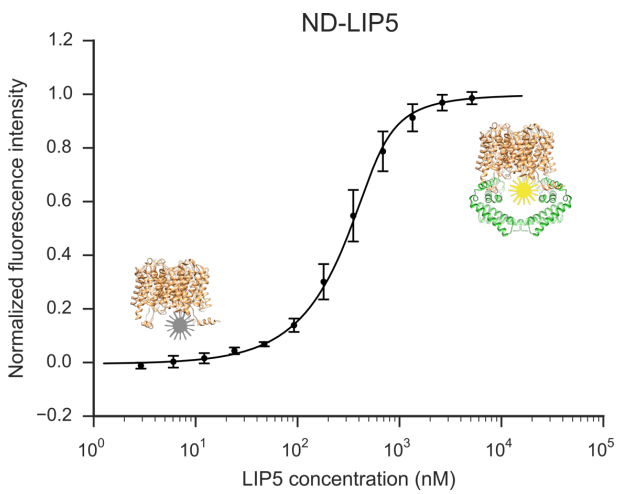

Figure 10. Binding curve constructed from a fluorescence quenching experiment. The dye Alexa^{488} is quenched when attached to AQP2. Upon additions of ND-LIP5 (x axis) the fluorescence increases (y axis) as the dye unquenches upon binding. The curve reaches a plateau of maximal fluorescence intensity when all binding sites on AQP2 are occupied.

Fluorescence quenching

Fluorescence is the ability of a fluorophore to absorb electromagnetic energy from light and this way reach an excited state. Upon transition to the ground state, which only takes a couple of nanoseconds, light is emitted. The fluorophore could be intrinsic – naturally occurring fluorescent amino acids tryptophan, tyrosine and phenylalanine. Alternatively, an artificial fluorescent probe (for example the Alexa dyes) or a tag (for example GFP) could be covalently or non-covalently attached to the studied protein. The absorption properties of fluorophores change depending on their environment. Quenching, that is the loss of fluorescence upon environmental change, could be either static, where the fluorophore forms a non-fluorescent complex with another molecule or dynamic, where the excited fluorophore transfers some of its energy to another molecule without emitting light. This phenomenon is successfully used to study protein conformational changes, folding/unfolding and ligand-binding [88].

In Paper II we have utilized the fact that the fluorescence of the fluorophore Alexa^{488} is partially quenched when attached to AQP2. When AQP2 binds LIP5 the environment of the fluorophore changes and the fluorescence is dequenched. This increase in fluorescence is dependent on concentration of LIP5, which allows us to construct a binding curve and determine the K_D (Figure 10).

Practically, a serial 2-fold dilution series of LIP5 was prepared. In a black quartz cuvette the labelled AQP2 was diluted to a final concentration as low as possible while the signal/noise ratio was still reasonable. Then the samples of LIP5 were sequentially added. After each addition the mixture was left to equilibrate for one minute and the fluorescence emitted at 515 nm upon excitation at 490 nm was recorded.

Microscale thermophoresis

While in electrophoresis proteins are known to migrate in an electric field according to their charge, during thermophoresis particles move along a temperature gradient. The exact mechanism underlying this movement is still not completely clear, evidence however points towards dependence on the size of the protein [89] and on the entropy of the solvation shell [90]. This dependence could be utilized in a binding experiment in order to detect the fraction of unbound and bound interacting partner in a sample.

The microscale thermophoresis (MST) experiment is performed in glass capillaries using instruments of the Monolith-series by Nanotemper. Typically, one of the interacting partners is fluorescently labelled (sometimes intrinsic fluorescence can be used) which allows tracking the movement of fluorescence along a temperature

gradient of a few °C caused by an IR laser. Similarly as during our fluorescence quenching experiments a 2-fold serial dilution of the unlabelled protein is prepared. The same amount of labelled protein is then added to each sample and those are loaded in capillaries. The much shorter light pathlength in capillaries compared to cuvettes allows for extremely low concentrations (in the range of tens of nM) of the labelled proteins to be used. This is a great advantage for proteins that are difficult to obtain in larger quantities. On the other hand, the common adsorption effects of protein sticking to the capillary walls and the price of the capillaries may be the limiting factors for usage of this method.

Before running the thermophoresis experiment itself the total fluorescence in each capillary needs to be measured. This is done during a capillary scan and ensures the correct interpretation of the results. Ideally, since all capillaries contain the same amount of labelled protein the total fluorescence of each capillary should be the same. Deviations from this could have several explanations. The proteins could for example be sticking to the tubes or the capillaries resulting in fewer molecules available in the solution. This sticking could be detected in the capillary scan itself as an unexpected distribution of fluorescence across the diameter of the capillary. Alternatively, the ligand binding to the labelled protein can quench or dequench the fluorescence. In this case no further thermophoretic experiments are necessary, the dissociation constant could be calculated directly from the dependence of the unlabelled protein concentration on the total fluorescence.

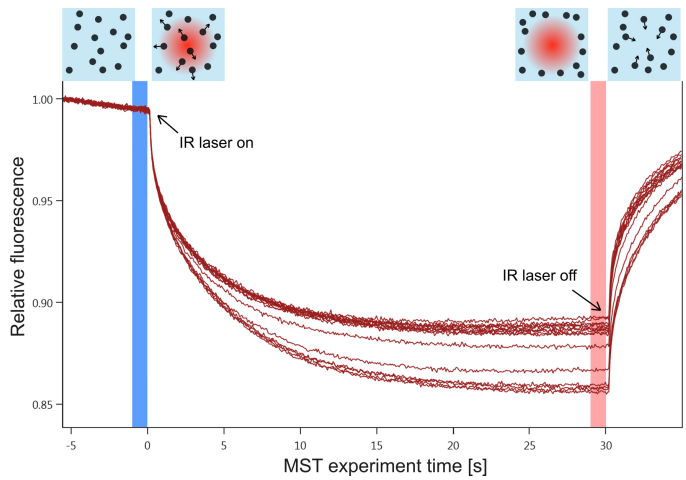

Figure 11. MST traces of one AQP5-PIP binding run. When the IR laser is turned on the labeled protein moves away from the heat based on the thermal gradient, resulting in a decrease in fluorescence. Once the laser is turned off the protein molecules diffuse back. For analysis, the fluorescence before heating (blue column) and during heating (red column) are used to determine the normalized change in fluorescence (ΔF_{norm}).

During the MST experiment a small area of the sample is heated and the change in fluorescence intensity in that spot is measured (typically over 30 seconds) as the molecules move either towards or away from the heat (Figure 11).

For analysis the change in fluorescence F_{norm} is defined as F_{hot}/F_{cold} – the average fluorescence during and before the heating. Plotting the normalized ΔF_{norm} of each of the points against the total concentration of the unlabelled protein in the respective capillary results in a binding curve.

In our laboratory we have used MST extensively to study the interactions between AQP2 and LIP5 (Paper I) , AQP5 and PIP (Paper IV) and AQP0 and CaM (Paper V).

Far western blot

During western blotting proteins are first separated using gel electrophoresis and transferred onto a blotting membrane. The specific protein is then detected using an antibody. Far western blot is a modification of this procedure that is used to study protein-protein interactions. After blotting, the proteins are renatured and the membrane is first incubated with a purified bait protein. This potential interaction partner is then detected using a specific antibody [91]. A comparison between various constructs can provide semi-quantitative answers abound parameters important for complex formation. In Paper I we have used this as a complimentary method in order to study the differences in binding of LIP5 to various phosphomimicking mutants of AQP2.

Nanodisc assembly

A neat way of reconstituting membrane proteins into a native-like environment is the use of nanodiscs. These small self-assembled discs are composed of a patch of phospholipid bilayer which is held together by a membrane scaffold protein (MSP) (Figure 12). One nanodisc would typically contain one copy of a membrane protein embedded in the lipid.

There are many kinds of MSPs varying in length and the presence of tags. The choice of MSP for a particular project therefore depends on size of the protein that should be reconstituted and on the selected purification method. The design of these scaffold proteins is based on nature's own apolipoprotein A-1, a protein responsible for transport of otherwise insoluble lipids through the bloodstream [92].

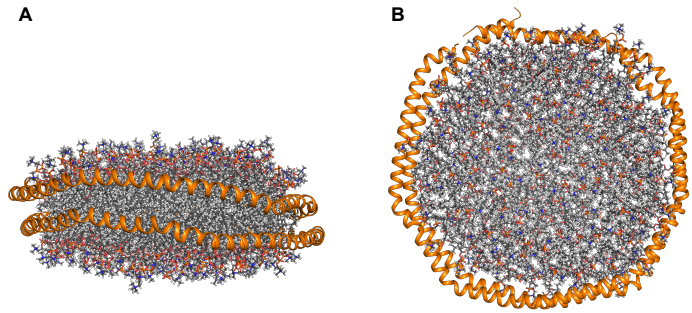

Figure 12. A nanodisc is a small disc consisting of a phospholipid bilayer (grey) heald together by a membrane scaffold protein (orange). Integral membrane proteins can be incorporated into the bilayer which mimics the native environment. **A.** side view; **B.** top view. (PDB code 6CLZ).

First, a membrane protein and a lipid, each solubilized in a detergent are mixed with an MSP. Then, Biobeads are added which strip the detergent off the protein and the lipid and the nanodiscs spontaneously assemble. The ratio of protein:lipid:MSP is the crucial parameter that needs to be optimized for each project. The proportion of lipids in the reaction will depend on the bilayer area of the resulting nanodiscs and also on how many lipid molecules will be displaced by the protein during the assembly, as compared to an empty nanodisc. Depending on particular phospholipid used the assembly is performed at various temperatures [93].

Nanodiscs containing the protein of interest need to be separated from the empty nanodiscs which inevitably form as well thanks to an excess of lipids and MSP used during the assembly. These two populations can be separated by SEC, if the size difference is large enough. In our case we needed to use the His-tag which was left on AQP2 but cleaved off the MSP in order to get rid of the empty nanodiscs. It is also possible to reconstitute the protein into nanodiscs while it is bound to Ni-NTA beads with its His-tag. After reconstitution the empty nanodiscs are simply washed away while the protein containing discs can be eluted with imidazole.

There are many parameters that could be optimized in order to increase the reconstitution yields. In my experience the concentrations and the ratios of all components as well as the amount of Biobeads added are critical. Other parameters that could be further optimized are: type of phospholipid, type of detergent used for phospholipid solubilization, type of MSP, temperature and time for the assembly [94].

The fact that protein is surrounded by phospholipid molecules, as it is in nature's membranes, allows the protein to assume its native conformation which might otherwise be disturbed by detergent. This way the purified protein is often stable for

much longer periods. We can also study any possible interactions between the protein and the lipids. Such sample can be used for light, X-ray or neutron scattering experiments where samples in detergents come with an unfavourable inhomogeneous background scattering [95]. Moreover, small hydrophobic molecules could be loaded into the phospholipid core and the nanodisc could serve as a potential drug delivery system [96].

In our case we have used nanodiscs to study the structure of the AQP2-LIP5 complex using cryogenic electron microscopy (cryo-EM). For protein in detergent it is often difficult to distinguish between empty micelles and micelles containing protein as those might have a similar size. Moreover, during protein concentration empty detergent micelles often get concentrated as well, which results in cryo-EM sample with empty micelles prevailing and a waste of the expensive microscopy time.

Unravelling protein structures with cryo-EM

The structure of all matter defines its function and its properties. Understanding how structure determines function can help us predict the binding of other proteins or to design drugs to fulfil a specific activity and treat specific diseases [97]. It is therefore of foremost importance to understand the atomic details of specific protein complexes.

For many years the most used method of membrane protein structure determination was X-ray crystallography. In the recent years many speak of a revolution in cryogenic electron microscopy (cryo-EM). The rapid advancement in both hardware (direct electron detectors) and software data processing has allowed cryo-EM to fast became one of the standard methods [98]. The record in highest resolution of a membrane protein solved by cryo-EM is currently held by a structure of voltage-gated sodium channel which reaches 2.6 Å [99].

X-ray crystallography is undergoing a revolution as well though, the number of structures with subatomic resolution is rapidly increasing thanks to development of new superbrilliant X-ray sources and new detectors [100]. For aquaporins the X-ray crystallography allowed determination of most currently known aquaporin structures, including for this thesis crucial structures of human AQP2 [10] and AQP5 [82].

The presence of detergent micelles surrounding purified membrane proteins is one of the largest sources of complications during structure determination by X-ray crystallography. The micelle can often weaken or hinder crystal contacts during crystallization. Moreover, obtaining protein quantities large enough for crystallization trials might be tricky. That is why membrane proteins are notoriously

hard to crystallize. Electron microscopy overcomes the crystallization step by visualizing individual protein particles and the amounts of protein needed are orders of magnitude lower.

Aquaporins are somewhat familiar with the use electrons for structural determination. Structures of several aquaporins were solved from 2D crystals using electron crystallography. Electrons interact with atoms more strongly than X-rays and the resulting diffraction pattern is much more easily interpreted. It is however not always possible to grow a thin crystalline plate of a protein. The only single particle EM-based model of an aquaporin is that of the AQP0-CaM complex at 25Å resolution [76].

Principle

The discovery in the beginning of 1980s that water can be cooled into a vitreous solid without the damaging crystalline ice formation was the key for development of cryo-EM. Until then only dry samples could be studied as water would evaporate during the high vacuum that electron microscopes require [101].

Here hundreds or thousands of 2D projection images are collected, each containing single particles in random orientation. These are then classified, averaged and oriented to reconstruct the 3D model of the particle. The larger the protein or the assembly is the more accurately it can be oriented during the 3D reconstruction and the better the resolution can be achieved [99]. The workflow is depicted in Figure 13. We have used cryo-EM in Paper III to study the complex of AQP2 (reconstituted in nanodiscs) with its interaction partner LIP5.

Sample preparation

Since thousands of particles will be averaged, the sample needs to be as homogeneous as possible. Thorough purification of the sample is therefore needed. A biochemically homogeneous sample (a symmetric peak in gel filtration) might not in fact be homogeneous in the microscope, owing to a potential conformational flexibility. In such case the buffer conditions should be screened to find an optimal buffer composition promoting homogeneity [102].

Membrane proteins require special handling before they can be studied and detergents are often used for solubilization. In such case it is recommended to use the high-concentration fraction from gel filtration without concentrating it in order to avoid the presence of empty detergent micelles in the sample as those contribute significantly to the background. Moreover, detergents lower the surface tension, making it more difficult to create very thin ice during plunge freezing [103].

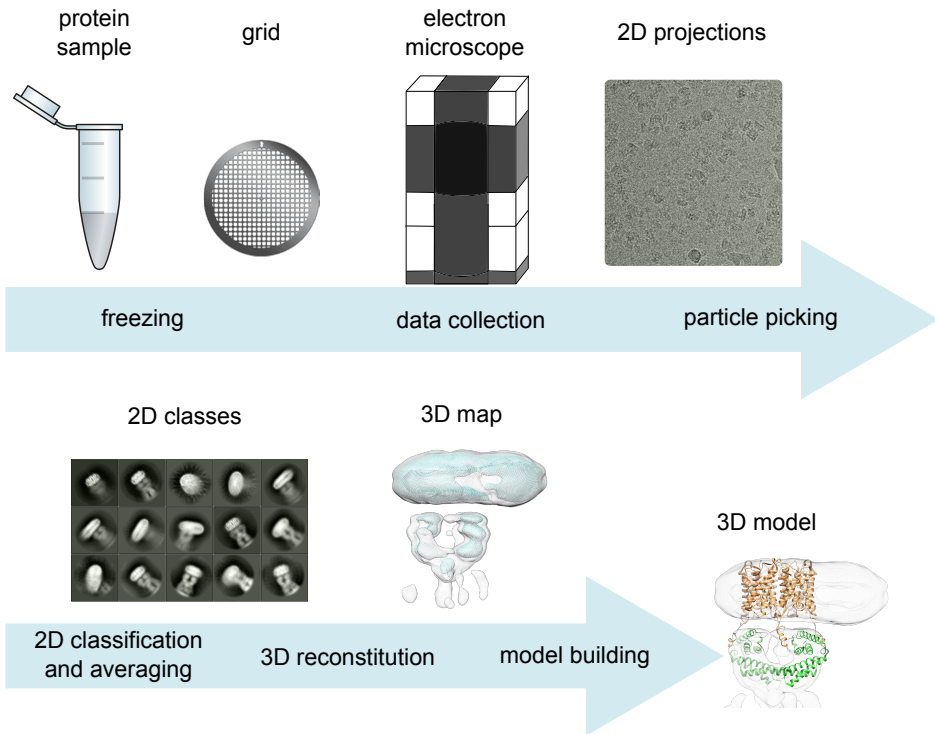

Figure 13. Cryo-EM workflow. (Images of the tube and the grid under the creative commons license.)

However, LMNG detergent in combination with gradient centrifugation for empty micelle removal has been successfully used [104]. Alternative solutions for membrane protein solubilization such as nanodiscs [94], amphipols [105] and SMALPs [106] are often beneficially used with single particle cryo-EM.

EM grids are small thin discs of metal with a grid of thin mesh. For cryo-EM the mesh is coated with a thin support layer of carbon which contains thousands of even smaller holes. The sample is deposited on top of the grid and typically an excess of liquid will be blotted away by a filter paper. The vitrified particles are imaged through the holes in the support film. Some samples can have very high affinity for the carbon film, which was the case for our sample as well. We solved the problem by simply increasing the concentration of the particles but one could also optimize the charge properties of the carbon film [102] or load the sample twice [103].

Even though the volume of sample that is used for one grid is very low, the total concentration of the protein needs to be relatively high. The smaller the particle is the higher concentration of it needs to be supplied to provide enough particle images for averaging and reconstitution. In our case the concentration needed to be as high as 3.5 mg/ml.

The sample homogeneity, purity and concentration can with advantage be assessed by negative stain electron microscopy (NS EM) since the grid is then prepared more quickly and easily. Moreover, no cooling is required so the imaging is often faster and the microscopy time is cheaper. In NS EM a salt of a heavy metal is deposited on top of the sample on the grid. This quickly dehydrates the sample and the heavy metal provides a contrast making the particles appear white on a dark background.

Plunge freezing

The negative stain EM is limited by resolution to approximately 20 Å. For achieving high resolution the contrast of the particle itself must be used. As explained earlier, for this the sample must be frozen in vitrified ice, in its native-like state. Plunge freezing is a method developed for exactly this purpose. For vitrification the sample must be frozen extremely rapidly (at a rate of 10^6 °C/s) so that the water molecules do not have a chance to order themselves into a crystallize state. This is achieved by dropping the blotted grid into a pool of liquid ethane. Before high resolution images can be obtained the ice thickness often needs to be optimized by varying the buffer composition and the blotting time before freezing. When already vitrified the sample-containing grids can be stored in standard liquid nitrogen [102].

Data collection

For the sample to be imaged on the grid the electrons need to pass through it. The electrons are generated in an electron gun and then detected for high resolution preferentially using a direct electron detector (DED). Collecting images in a movie-mode allows the electron dose to be divided into several frames. These frames are then aligned, while compensating for sample drift, and averaged to create a complete image [103].

The electron dose needs to be very small in order to avoid radiation damage of the sample. The contrast of the resulting images is therefore not very high. This can be improved by defocusing the microscope and increasing the contrast at a cost of losing some resolution [102].

Data analysis

Before the data can be analysed the raw images need to be corrected for a myriad of effects, for example the spherical aberration of the microscope, the defocus and others [103]. Selected good micrographs are then subjected to particle picking which is done mostly by an automatic algorithm, often with some manual elements. Each

picked particle is then iteratively aligned and grouped into homogeneous subsets. The stacks containing particles imaged in the same orientation are averaged and a 3D model is constructed. The initial map is then refined to obtain the final map. Sometimes particles tend to assume preferred orientations, presumably due to interaction with the water/air interface. This creates a problem for the 3D reconstitution.

Many samples are not entirely structurally homogeneous, for example by containing several populations with varying conformation or stoichiometry. 3D multi-reference alignment can cluster all images into a given number of groups and create new 3D reconstructions. This should be guided by examining the local variability in the map [103].

Validation of the structures

In cryo-EM, resolution is understood as the self-consistency of the result [107]. The most common resolution measure is the Fourier shell correlation (FSC) curve. The dataset is randomly split into two halves and each half is processed independently. The FSC curve plots the correlation coefficients between the two maps against corresponding resolution shells of the reciprocal space [103]. When the FSC curve is close to 1 a strong similarity between the two halves of the dataset is present, while values close to 0 indicate no similarity. Most often, FSC would decrease with the increasing spatial frequency. If the resolution is reported as a single number it corresponds to the maximum spatial frequency where the structure is still considered reliable. What is considered reliable can be rather subjective and many methods of cut-off based on FSC or signal-to-noise ratio exist. Rather than using the resolution the quality of the data should be judged by the shape of the entire FSC curve [107] or using the directional resolution assessment in 3D-FSC [108].

Depending on the resolution reached the overall validation strategy differs. For low-resolution maps (>10 Å) only the overall shape can be seen and docking of X-ray structures is unreliable. These maps should be validated by additional tilt experiments. Medium-resolution maps (4-10 Å) reveal details of secondary structures and can therefore be validated when the shape agrees with docked X-ray structures, if available. High-resolution maps allow for polypeptide backbone tracing and show density for most side chains [103].

Regulation of water transport by phosphorylation (Paper I and V)

In these two papers we have studied the effect of protein phosphorylation by introducing phosphomimicking mutations. The mutants of AQP2 were probed for stability and binding affinity toward LIP5 in order to understand how phosphorylation controls AQP2 trafficking. In AQP2 four residues were individually mutated to glutamic acid: Ser 256, Ser 261, Ser 264 and Thr 269. We have also created a double mutant S256E/T269E because this double phosphorylation occurs naturally and is common in AQP2 at the apical membrane.

Similarly, all three known phosphorylation sites on AQP0 C-terminus – Ser 229, Ser 231 and Ser 235 – were individually mutated to aspartic acid and the resulting constructs were purified. These phosphomimicking mutants were probed for their water permeability, their sensitivity to CaM/Ca^{2+}-induced gating and their binding affinity towards CaM. This helped us understand how phosphorylation regulates CaM-dependent AQP0 gating.

Post-translational modifications

The yeast *Pichia pastoris*, which was used to express both AQP0 and AQP2, is capable of higher eukaryotic protein post-translational modifications (PTMs) [84]. Since it is the effect of PTMs that we are studying in these two papers the PTM status of our samples needs to be uncovered before any experiment can take place.

Mass spectrometry analysis of trypsin-digested AQP2 showed phosphorylation of Ser 256, Ser 261 and Ser 264 in all possible combinations. Therefore, an efficient cleavage of these phosphoryl groups was necessary in order to study the effect of phosphomimicking mutations on the AQP2 functionality and LIP5-binding. Dephosphorylation was performed using alkaline phosphatase and the effect of the treatment was confirmed with a western blot using a phosphorylation-specific tag.

Contrarily to AQP2, AQP0 was not phosphorylated when expressed in *Pichia*. Upon maturation in the eye lens, the AQP0 C-terminus (where the CaM binding site is

located) is cleaved off [109]. We used linear-mode MALDI mass spectrometry to determine the exact size of our recombinant AQP0 sample. The spectrum shows one predominant peak at 28955.4 ± 9.2 Da (n=3) (Figure 14) which corresponds to the size of full-length AQP0 (28944.6 Da). This confirms that the protein in our sample is not truncated and can be used to study the binding to CaM.

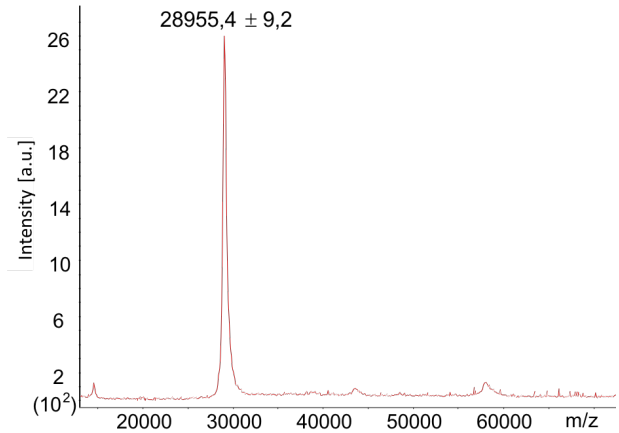

Figure 14. Linear MALDI spectrum of our AQP0 sample shows a single peak at 28955.4 ± 9.2 which corresponds well to the predicted size of full-length AQP0. This confirms that the protein is not truncated.

Protein stability and functionality

In order to study the possible structural changes and shifts in AQP2 stability caused by the individual phosphorylation each purified mutant was tested using circular dichroism spectroscopy. The overall fold of all AQP2 mutants was very similar, however the thermal stability was significantly reduced for S256E, S261E, S264E and S256E/T269E while the dephosphorylated wild-type AQP2 displayed the highest stability.

AQP0 was reconstituted in proteoliposomes and the water permeability (P_f) was tested by a shrinkage assay upon rapid mixing with a hyperosmotic solution. We could conclude that our recombinantly expressed AQP0 is a functional water channel. Only upon incubation with both CaM and Ca^{2+}, the water permeability was reduced more than 2-fold, confirming that the direct binding of CaM closes the channel.

The effect of AQP0 phosphorylation on CaM-mediated gating

In this study we aimed to understand how the cell uses phosphorylation to regulate the water transport across the plasma membrane. In liposomes the water permeability of all three phosphomimicking mutants was comparable to the one of the AQP0 wild-type. However, with the presence of CaM/Ca^{2+}, none of the mutated channels could be closed and the water permeability remained unchanged.

We used MST to study the binding of these mutants to CaM in the presence of Ca^{2+}. Previously, the wild-type AQP0 could bind CaM in a cooperative manner with K_{d1} of 40 μM and K_{d2} of 2.5 μM [110]. As expected for S229D and S235D the binding to CaM was completely abolished. However, S231D could still bind to CaM with an affinity of 1.49 ± 0.48 μM which is similar to the wild-type AQP0. This was somewhat surprising because we have observed no CaM sensitivity during the functional studies of this construct. Also, previous studies with short peptides containing the CaM binding site showed that once either of the sites were phosphorylated the binding to CaM was completely abolished [77]. In MST the binding curve had an opposite direction than the one for wild-type. Moreover, the data could be only fitted with a one-to-one binding model, not the cooperative two-binding-sites model which fits the wild-type data. We therefore concluded that S231D is still able to bind CaM but in a different binding mode which does not result in channel closure. The physiological relevance of this binding is not clear and will need to be studied further.

The effect of AQP2 phosphorylation on LIP5 binding

In Paper I we have studied the binding of LIP5 to AQP2 using MST and far-western blot. The quantitative method MST revealed that the interaction had an affinity of 191 ± 43 nM for dephosphorylated AQP2. As a negative control AQP4 was probed for binding to LIP5 which did not result in a binding curve. Interestingly, removing the distal C-terminus of AQP2 (containing the phosphorylation sites) while keeping the LIP5 binding site intact reduced the LIP5 binding almost 20-fold (3.63 ± 0.44 μM, construct P242Stop on Figure 15) and the same could be observed in the far-western blot. To elucidate the mechanism by which the distal C-terminus affects the interaction we have tested the binding of corresponding distal C-terminal phosphorylated peptides to both AQP2 and LIP5. The lack of this binding suggests that the distal C-terminus allosterically modulates the AQP2-LIP5 complexation.

The main goal of this paper was to investigate the effect of AQP2 phosphorylation on the interaction with LIP5. LIP5 is known to be involved in the MVB formation and binding to AQP2 is therefore suggested to target the protein for degradation or exosomal secretion [41,111]. We also know that AQP2 is differentially phosphorylated depending on the subcellular localization [29].

All previously mentioned phosphomimicking mutants were dephosphorylated, purified and probed for interaction with LIP5 using MST. The phosphomimicking residues decreased the binding affinity towards LIP5 in most cases (Figure 15). Wild-type dephosphorylated AQP2 showed the highest affinity for LIP5 (191 ± 43 nM). This was expected because at this state the protein exists after the ESCRT complexes recognize and cleave off the K270 ubiquitination and the protein is ready to be internalized to MVB. S264E bound LIP5 with a similar affinity as the wild-type (278 ± 49 nM). The phosphorylation of S264 was suggested to play a role in excretion of AQP2 in exosomes [33]. Exosomes originate from MVBs therefore the interaction of LIP5 with this form of AQP2 is also expected.

The lowest affinity was seen for S256E (1.00 ± 0.25 μM), a construct mimicking the phosphorylation that is necessary for targeting to the apical membrane [27]. S261E, T269E and S256E/T269E all showed decreased binding to LIP5 (745 ± 141 nM, 721 ± 55 nM, 652 ± 62 nM, respectively). The phosphorylation of S261 is associated with protein retention in intracellular vesicles [32] and the phosphorylation of T269 happens once the protein is to be stabilized in the apical membrane [31]. It is reasonable to expect that LIP5 would not bind AQP2 in these stages *in vivo*. Overall, our results can be very well explained by the previous observations of differentially phosphorylated AQP2 in different sub-cellular compartments.

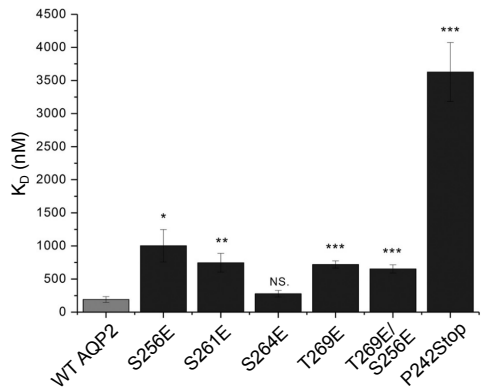

Figure 15. Binding affinities of the interaction between the individual AQP2 phosphomimicking mutants and LIP5 resulting from the MST experiments. For each mutant the data were obtained from three individual dilution series. Significance between the affinities for the mutants and the wild-type was tested using a Z-test for two popluation means (*, p<0.05; **, p<0.01; ***, p<0.001; NS. means no significance was found). Figure reproduced from [112].

Structure of the AQP2-LIP5 complex (Paper II and III)

Point mutations of the binding site give insight into the binding mode (Paper II)

From previous studies we know that AQP2 co-localizes with LIP5 in the principal cells of the kidney collecting duct. We also know that the binding occurs between the amino acids 230 and 242 on the C-terminus of AQP2 [41].

In Paper II we have investigated the structural details of this interaction. First, we identified that the binding site is located at the N-terminal domain of LIP5. This was done using a fluorescence quenching binding experiment. We measured the binding affinity of AQP2 to the full-length LIP5 (FL-LIP5) and to the isolated N-terminal domain of LIP5 (ND-LIP5). K_D was determined to be 237 ± 66 nM and 64 ± 34 nM, respectively.

Based on this result we postulated that the binding site might be located on the MIT domain of LIP5. The fact that the C-terminal helix of AQP2 contains residues corresponding to a consensus MIM-motif further supports this. Figure 16 shows an overlay of the MIM-motif in AQP2 and the MIM-motif in ESCRT-III peptide CHMP1B.

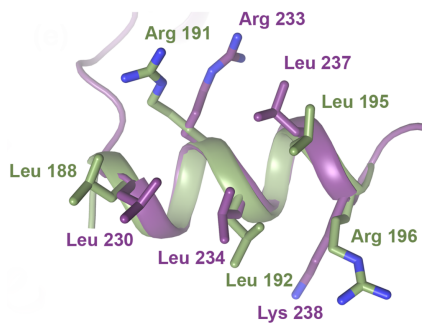

Figure 16. Overlay of the MIM-motifs of CHMP1B (green) and of AQP2 (purple) shows a match in the positions of the side chains. Figure reproduced from [35].

To get a structural idea about what the binding interface might look like we performed an *in silico* molecular docking using the online HADDOCK server [113]. The residues on the LIP5 MIT domain known to interact with CHMP1B and the AQP2 MIM-motif were selected to drive the docking. Of the many resulting solutions two were selected based on the highest docking score and the similarity to the way how LIP5 binds to CHMP1B (Figure 17, left).

In these two models the binding site on LIP5 remains the same but the C-terminal helix of AQP2 binds from opposite directions. Cluster 3 (Figure 17B) was the model that was the most similar to the way LIP5 binds CHMP1B, both in the direction of the helix and the amino acid interactions. Specifically, Arg 233 of AQP2 creates hydrogen bonds with Asp 65 and Glu 68 of LIP5 in the same way as the corresponding Arg 191 of CHMP1B does.

To be able to verify the docking on real molecules and to distinguish between these two models we created alanine point mutants of the individual residues involved in the binding interface of these two docking models. All LIP5 and AQP2 mutants were individually expressed and purified and the binding to their corresponding wild-type partner was characterized using fluorescence spectroscopy.

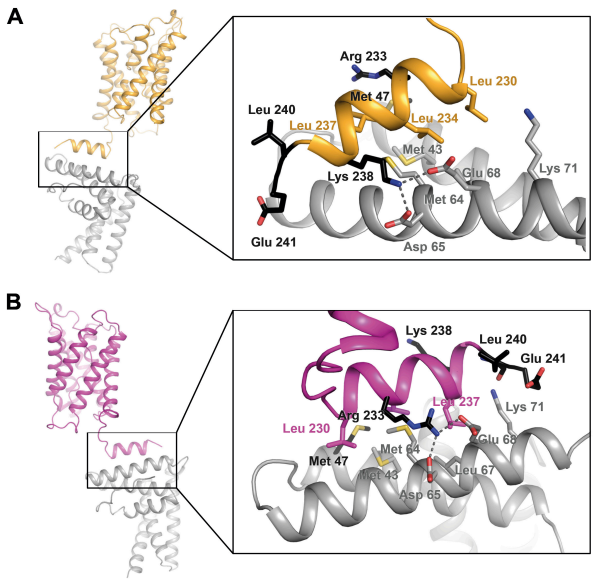

Figure 17. The two best computational docking models of the AQP2-LIP5 interaction. **A.** Cluster 2; **B.** Cluster 3. All labeled residues were mutated to alanines and the mutants were tested for binding affinity. Residues highlighted in black proved to be important for the interaction. Figure adapted from [35].

On AQP2 the mutation of Arg 233, Lys 238 and Glu 241 to alanines caused a significant decrease in binding affinity (486.8 ± 75.7 nM, 552.0 ± 151.7 nM and

699.6 ± 100.7 nM, respectively) while the mutation of Leu 240 abolished the interaction completely. On LIP5 the mutation of Met 47 decreased the binding affinity (463.1 ± 81.1 nM). These residues are highlighted in black in Figure 17. Four out of these five mutants are directly involved in the binding in Cluster 3, while in Cluster 2 these are pointing away. We therefore concluded that Cluster 3 represents the most probable binding mode. Overall, our results suggest that the binding between LIP5 and AQP2 structurally resembles the binding between LIP5 and CHMP1B. This could mean that CHMP1B competes with the cargo protein, in this case AQP2, over binding to LIP5.

Binding mode from cryo-EM perspective (Paper III)

For our single particle cryo-EM studies AQP2 was purified and reconstituted into nanodiscs. These were then mixed with ND-LIP5, the complex was concentrated and vitrified on carbon grids. The datasets were collected on a Titan Krios microscope with a Falcon 3EC direct electron detector. The micrographs show particles evenly distributed in the holes (Figure 18A). Two types of particles can be seen, one type containing one nanodisc with some density below it and the second type consisting of a sandwich arrangement of two nanodiscs with density in between them (Figure 18B). This is probably caused by an unphysiological oligomerization of ND-LIP5 due to the truncation. During particle picking we have selected single nanodiscs no matter whether they were part of the single or the double particles. Upon 2D classification (Figure 18C) it became obvious that we had a strongly preferred orientation of the particles in the ice and collecting an additional 30° tilt dataset only partly alleviated this problem.

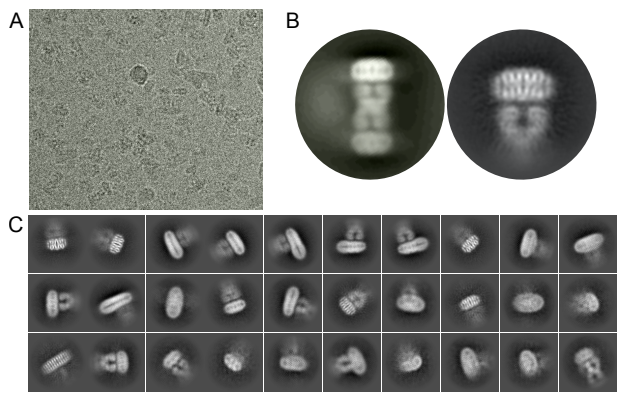

Figure 18. Cryo-EM data analysis. **A.** Raw micrograph; **B.** Averaged double particle in a sandwich arrangement in comparison with a single particle; **C.** Thirty of the most abundant 2D classes, each containing thousands or tens of thousands averaged particles.

The final resolution of the constructed 3D map is therefore only 8 Å although the side views show many details and the particles possess the capacity for higher resolution.

The cryo-EM density map shows a clear ellipsoidal structure of the nanodisc where the structure of AQP2 (PDB code 4NEF) could be docked based on a circular bulge on top of the disc and a presence of a dip where the central pore is located. Below the disc four clear densities can be seen, two of which are large, bi-lobar, and two of which are much smaller (Figure 19A). Two molecules of ND-LIP5 (PDB code 4TXQ) fit well into the larger densities and are positioned diagonally below AQP2 (Figure 19B). The two smaller densities might present an additional ND-LIP5 binding sites with much lower occupancy, resulting from the 2D averaging of the particles. Below this some additional densities could be observed, possibly arising from the oligomerization of ND-LIP5 in the sandwich arrangement which was partly included in the box during particle picking.

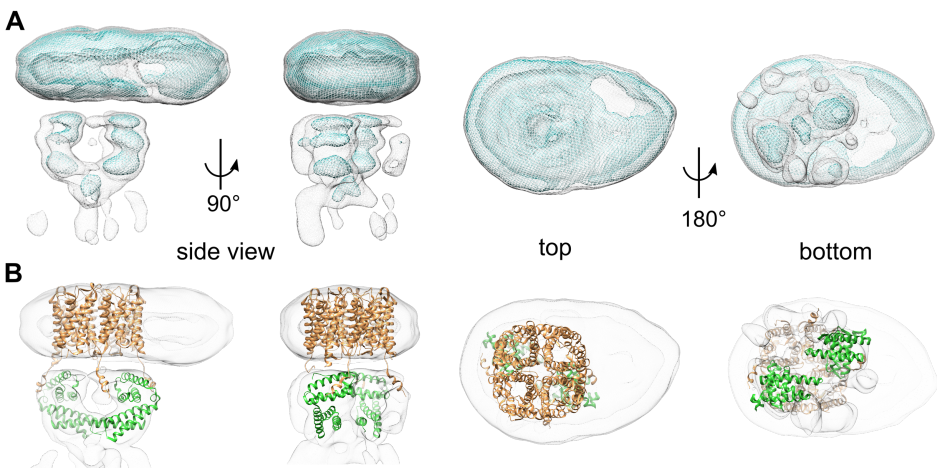

Figure 19. A. Cryo-EM density map of the AQP2-LIP5 complex. Grey mesh – level of confidence corresponding to the size of the proteins to be docked (sigma level 3.4), blue mesh – high level of confidence (sigma level 4.7) **B.** Model of the complex based on rigid body docking.

Upon rigid body docking in UCSF Chimera [114] it is striking how well the complex fits our results from Paper II. Indeed, the helices 2 and 3 of ND-LIP5 were pointing directly towards the short C-terminal helix of AQP2 (Figure 20) in an orientation resembling our docking Cluster 3. When docking ND-LIP5 with the interacting peptide CHMP1B, this peptide is located only 10 Å away from the C-terminal helix of AQP2. Because of the unusual flexibility of this helix known from the crystal structure [10], we went ahead and manually moved this helix to match the position of CHMP1B (Figure 20). This results in a model when the two ND-LIP5 molecules are rather closer together, right below the nanodisc, possibly

stabilized by an interaction between their sixth helices. This hypothesis is strengthened by the presence of continuous density between the lower side of the ND-LIP5 densities. The AQP2 construct contains additional 32 residues which are not part of the crystal structure used for docking. Unfortunately, the resolution of the cryo-EM map is too low to be able to assign some position to this rest of the C-terminus.

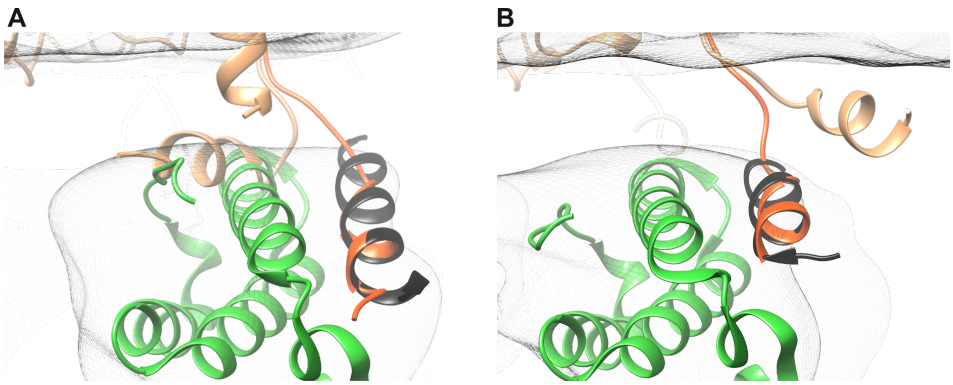

Figure 20. Close up of the AQP2-LIP5 binding interface in our cryo-EM model. The two interaction sites shown in **A.** and **B.** correspond to the C-termini of monomers A and B in the crystal structure of human AQP2 (sandy brown, PDB code 4NEF) which was used for modelling. Neither of the two C-termini are in the correct location for their MIM-motifs to interact with LIP5 (green), as illustrated by the CHMP1B peptide in black (PDB code 4TXQ). The short C-terminal helix of AQP2 was moved to match the binding site (orange).

Stoichiometry (Paper II and III)

Since the beginning of the project the stoichiometry of the AQP2-LIP5 complex was drawing our interest. Knowing that the binding site is located on the short C-terminal helix of AQP2 means that there are four possible binding sites on each tetramer. Moreover, *in vivo* full-length LIP5 dimerizes through its C-terminal domain [37], therefore exposing two N-terminal domains for the interaction.

We first studied the stoichiometry of the complexation using fluorescence quenching in Paper II. When using concentrations of labelled AQP2 well above the K_D and titrating with LIP5 until and beyond the saturation point a typical kink could be observed when plotting the fluorescence intensity against the LIP5:AQP2 ratio (Figure 21). The molar ratio, determined from the saturation point was 0.42 ± 0.08 for FL-LIP5 and 0.29 ± 0.07 for ND-LIP5. Statistical T-test revealed no significant difference between these two. On average a maximum of two molecules of LIP5 (full-length or truncated) are expected to bind to one AQP2 tetramer.

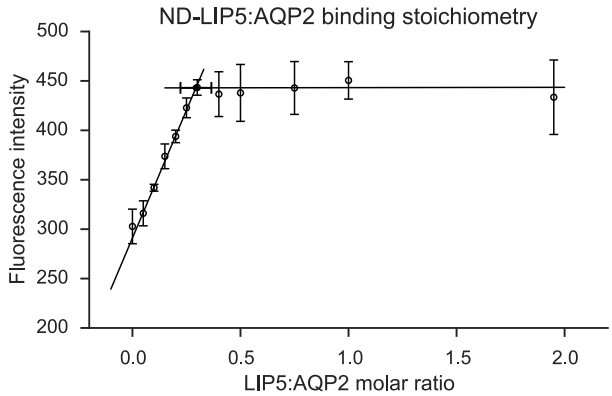

Figure 21. Fluorescence quenching experiments between AQP2 and ND-LIP5 at high concentrations of labeled AQP2 resulted in a clear kink at 0.29 ± 0.07 molar ratio ND-LIP5:AQP2. Figure reproduced from [35].

The stoichiometry was then confirmed in Paper III as the cryo-EM map of the complex contains two large densities for ND-LIP5 bound to each AQP2 tetramer.

Characterization of the AQP5-PIP complex (Paper IV)

Previous studies suggest that normal AQP5 trafficking is dependent on a presence of a small regulatory protein PIP. A peptide corresponding to residues 251-265 of the AQP5 C-terminus was used to pull-down PIP from a native tissue [51]. In Paper IV we have recombinantly expressed and purified both proteins and characterized their interaction.

PIP is inhomogeneously glycosylated

Since the glycosylation status of PIP was previously identified to have an effect on the interaction with CD4 [115] we made sure to test whether our PIP, expressed and secreted by *Pichia pastoris*, was glycosylated. Part of the purified PIP sample was treated with an enzyme PNGase F. Both treated and untreated samples were run on SDS-PAGE and western blot, detecting the His-tag present on the C-terminus. What appeared as a smear around 20 kDa before treatment became four clear bands after the treatment. The western blot detected PIP at 12, 13, 14 and 16 kDa. We therefore concluded that in our sample PIP is inhomogeneously glycosylated. Moreover, several species of PIP are present, probably as a result of inefficient cleavage of the secretion signal, a phenomenon well described for IgG [116].

Full-length AQP5 binds PIP

His-tagged PIP was bound to a nickel-affinity column and full-length AQP5 was allowed to pass through. After thorough washing the presence of AQP5 in the eluate would confirm the interaction. The 300mM and 400mM imidazole eluates were concentrated and run on an SDS-PAGE gel with total protein detection, selective glycoprotein detection and on anti-His western blot.

On the SDS-PAGE gels AQP5 shows a typical laddering due to many stable oligomeric states. Interestingly, this laddering was also seen in both elution fractions but it was slightly increased in size. Moreover, the western blot which only detects PIP shows this laddering as well. This confirms that full length AQP5 binds to PIP. Moreover, in the 400mM imidazole elution the signal from the His-tag is very strong however the glycosylation staining is weak. This might suggest that during the binding the glycans are part of the interaction interface and therefore not available for the dye.

After confirming the interaction, we embarked to quantify the binding using MST, in a similar way as we did for AQP2-LIP5 and AQP0-CaM in Papers I and V. Fluorescently labelled PIP was titrated with AQP5 and the dataset in triplicates was fitted with the Hill equation (Figure 22). Binding affinity was determined to be 0.57 ± 0.12 μM and the Hill coefficient is 2.24 ± 0.66 which indicates positive cooperativity of the binding.

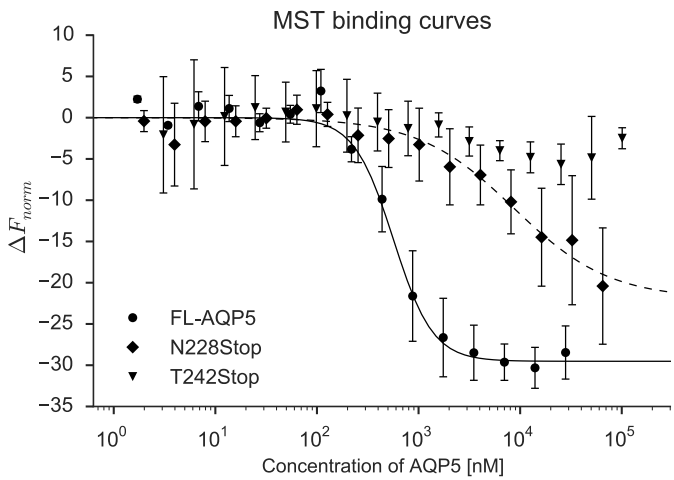

Figure 22. Binding curves from the MST experiments with PIP and three AQP5 constructs of different lengths of the C-terminus. The full-length AQP5 binds with an affinity of 0.57 ± 0.12 μM while the binding of the two truncated constructs is impaired.

Since the binding site was suggested to be on the C-terminus of AQP5, we created two additional constructs with C-terminal truncations. N228Stop is missing the entire C-terminus, including the short α-helix (residues 231-241), which is conserved in mammalian aquaporins and is a common site for interactions with regulatory proteins [8,117]. The second construct, T242Stop, preserves this helix but lacks the downstream disordered terminus where PIP was suggested to bind. As expected, both constructs exhibited severely impaired binding to PIP. Instead of a binding curve N228Stop showed a slowly decreasing trend without reaching any

plateau which likely represents unspecific binding at high concentrations. For T242Stop the amplitude was extremely small and we therefore concluded no binding (Figure 22). Indeed it is the distant C-terminus that mediates the binding to PIP, rather than the short helix, which is in agreement with a previous study [51].

Stoichiometry

Because of the positive cooperativity of the binding between PIP and full-length AQP5 the natural next step was to elucidate the stoichiometry of the complexation. For this we have also used MST but with concentrations of labelled PIP well above the K_D. At a concentration of AQP5 where all binding sites were saturated a characteristic kink could be observed on the plot (Figure 23). This kink corresponds to a monomeric molar ratio of AQP5:PIP of 5.5 ± 1.8. We interpret this ratio as one molecule of PIP binding to AQP5 tetramer since AQP5 is known to always occur as a homotetramer.

Even if only one PIP binds to an AQP5 tetramer it is still possible that it binds to two or more C-termini, as supported by the positive cooperativity of the binding. It is simple to imagine several C-termini binding PIP from different sides. This is the case for binding of CaM to AQP0 where two copies of AQP0 C-termini bind to the same molecule of CaM [76], also in a cooperative way [110].

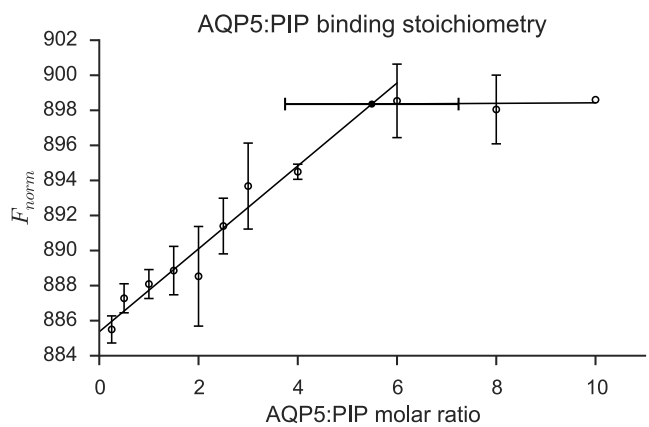

Figure 23. MST experiment of the stoichiometry for the binding of AQP5 and PIP at high concentrations of labeled PIP resulted in a kink at 5.5 ± 1.8 molar ratio AQP5:PIP.

Discussion

The common mechanism of aquaporin regulation

Let us look at what the three isoforms of aquaporins studied in this thesis have in common. Apart from the obvious, like the common tetrameric arrangement, the common α-helical fold and the common water channel function, these three also share the ability to be quickly and highly operatively regulated based on the cellular needs. Various triggers prompt the regulation [19,118] where the regulatory signal is carried out by binding of other proteins [8]. This binding needs to be specific but only transient to be able to dynamically regulate the hydration levels. A second layer, a regulation of regulation, constitute post-translational modifications, specifically phosphorylation [9]. AQP0, AQP2 and AQP5 can all be phosphorylated, most commonly on the C-terminus [9]. In AQP0 this affects the binding of calmodulin and therefore the regulation by gating. In AQP2, different phosphorylation sites act as a code for trafficking between different sub-cellular compartments which is mediated by protein-protein interactions. The phosphorylation status of AQP2 was previously found to play a role in binding of various other regulatory proteins like Hsp70, clathrin, protein phosphatase 1c or G-actin [119,120]. The phosphorylation also affects binding to its regulatory protein LIP5 in a pathway leading to AQP2 degradation. And finally, for AQP5, phosphorylation is also associated with regulation of trafficking [22]. Whether this is done through affecting the binding to PIP or other protein is currently not known but seems plausible. In AQP0 the phosphorylation sites are part of the short C-terminal helix while in AQP2 those are located at the distant C-terminus. AQP5 ranks somewhere in between, sharing two of the phosphorylation sites with AQP0 and one with AQP2, in addition to two unique sites in the cytoplasmic loop D.

The combination of trigger, phosphorylation and protein-protein interactions possibly establishes a common mechanism of regulation for all aquaporins. To date, apart from the proteins studied in this thesis, the trafficking of AQP1, AQP4 and even some plant aquaporins have been shown to be regulated by phosphorylation [9]. Moreover, the kinases and phosphatases involved in the processes are themselves regulated which adds another layer of complexity to the system. To be able to fully

understand the cascades of aquaporin regulation, functional studies in whole cells will be necessary, which was not part of this thesis.

The cytoplasmic C-terminal helix received a lot of attention in this thesis. Built by approximately 10-12 residues, it is very conserved between all three isoforms, implying the importance of this region (Figure 24). The orientation of this helix is conserved in most mammalian aquaporins that have been structurally characterized, the notable exception being AQP2 in which it assumes different conformations in each monomer with respect to the tetramer. The helix is of a clear amphipathic character with the hydrophobic side involved in interactions with CaM/LIP5 [110]. An interaction partner for AQP5 which would bind here has not yet been discovered but it can be expected that even in AQP5 this regulation mechanism would be employed. From the sequence alignment (Figure 24) we can see that the arginine and lysine on AQP2 that we have identified to be key for interaction with LIP5 are both conserved in AQP0 and AQP5. Moreover in AQP0 two of the leucines from the MIM-motif are also conserved. This opens a new question of whether AQP0 and AQP5 could bind LIP5 and whether such interaction would be physiologically relevant.

Figure 24. Sequence alignment of the segment corresponding to the short conserved C-terminal helix. Known phosphorylation sites are marked in blue [9]. Key residues from the 1-8-14 calmodulin-binding motif are marked in yellow [77]. Key residues for binding LIP5 are marked in green [35].

Since we have no 3D structural information about the distal C-terminus, this part of the protein could sometimes be overlooked. Nevertheless, it contains additional 27-35 residues whose conformation is flexible and which are potentially available for interactions. The importance of this region is demonstrated in AQP5 as it is here PIP binds, not at the short helix, as we showed in Paper IV. The fact that PIP does not bind to the short helix was no surprise when looking at the structure. PIP consists entirely of β-sheets while the other two interaction partners LIP5 and CaM are helical. Moreover, the distal C-terminus of AQP2 contains phosphorylation sites which allosterically modulate the binding of the short helix to LIP5. The binding is impaired when the distal C-terminus is deleted, further indicating the importance of this region. AQP5 as well AQP4 also contain distal phosphorylation sites which modulate trafficking of the proteins [9].

Story 1: AQP2-LIP5

The primary binding sites on both AQP2 and LIP5 and the involvement of specific residues within the MIT/MIM motifs were studied in Paper II. Curiously, the binding affinity of the isolated domain was higher than the one of the full-length protein (64 ± 34 nM and 237 ± 66 nM respectively). The reason for this is unresolved, however, steric constrains and isolating the domain out of its full-length context might contribute to this observation.

The results of our stoichiometry experiments in Paper II, confirmed by the cryo-EM map of the complex from Paper III are adding an interesting perspective. In both studies we see two molecules of LIP5 binding per one AQP2 tetramer. LIP5 is known to dimerize via its C-terminal domain [37] and each dimer therefore has two N-terminal domains available for interaction. Different ESCRT-III components bind LIP5 during the last steps of the MVB formation and regulate the ability of LIP5 to activate Vps4 [40]. In our studies we have shown that LIP5 also directly binds the cargo protein AQP2. Potentially, the LIP5 dimer could attach to CHMP1B with one N-terminal domain while holding the cargo protein AQP2 with the other one (Figure 25). The process of cargo protein incorporation into the MVBs could be driven by a competition over the binding to LIP5, however the particular order of binding events is currently not known. The activation of Vps4 ATPase by binding of both LIP5 domains causes the disassembly of ESCRT-III and the final membrane fission [38]. The fact that each AQP2 tetramer can bind both of the N-terminal domains from the dimerized LIP5 at the same time may be important for an effective disattachment of the complex from the sorting machinery at the point of MVB vesicle formation. The whole AQP2-LIP5 complex can be enclosed in the vesicle as both proteins were reported in a proteomic analysis of exosomes from human urine [121].

This model of the process is surely still highly simplified and the reality is probably more intricate due to the fact that Vps4 forms a hexameric ring with a potential to bind up to six LIP5 dimers. The Vps4 also contains a MIT domain through which it binds the rest of the components of the ESCRT-III but it could also compete over the binding of the LIP5 N-terminal domain [40]. LIP5 is also known to bind to other components of the ESCRT-III complex, for example to IST1 [42] or CHMP5 [40]. Competition binding experiments will be needed to elucidate the causality and the order of these binding events and therefore of the whole process or formation of MVB vesicles. Pull-down assay and bioinformatics studies could provide more information on how general or specific LIP5 binding is for recruiting membrane proteins into MVBs.

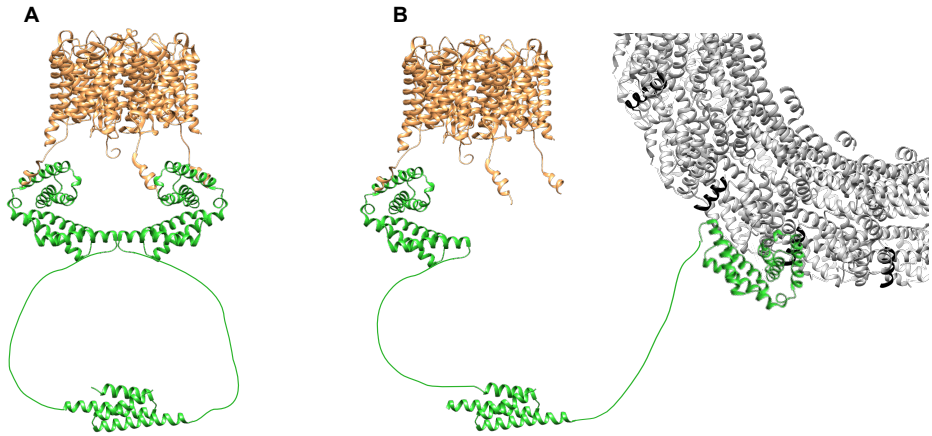

Figure 25. Schematic representation of binding competition over LIP5 N-terminal domain. **A.** A dimer of full-length LIP5 (PDB codes 4TXQ and 2RKL, green) binds two monomers of AQP2 (PDB code 4NEF, orange) within the same tetramer **B.** A LIP5 dimer binds AQP2 with one of the N-terminal domains and CHMP1B (PDB code 6E8G, grey) of the ESCRT-III fibre with the other N-terminal domain. Helices corresponding to the binding site on CHMP1B are highlighted in black.

Considering that on AQP2 the phosphorylation sites are not located within the LIP5 binding site, we hypothesised that this phosphorylation might either allosterically change the conformation of the C-terminal helix, which would impair the binding, or that there is another binding site located at the disordered C-terminus, which is blocked when phosphorylated. The latter is supported by our results from the MST measurements: A truncated AQP2 which keeps the LIP5-binding site but misses all phosphorylation sites binds LIP5 with 20-fold lower affinity than the wild-type. On the other hand, peptides corresponding to the distal C-terminus of AQP2 would not independently bind to LIP5 no matter their phosphorylation status. Evidently, the entire C-terminus is important for the interaction with different parts having different roles in the complexation.

The distal C-terminus is still escaping our sight, as intrinsically disordered proteins or parts of proteins traditionally have done. Due to their flexible nature both X-ray crystallography and cryo-EM have difficulties in characterizing the features. Here, NMR spectroscopy becomes a very useful method. Moreover, intrinsically disordered proteins can be at least partially captured and stabilized when bound to another protein. Then, distances could be measured using cross-linking mass spectrometry or fluorescence resonance energy transfer and structure determination can shed light to the interacting features, providing that the resolution is high enough. Some of these methods could be used in the future to shine more light onto the role of the distal C-terminus in AQP2 interactions.

In our cryo-EM structure of the AQP2-LIP5 complex we have used only the N-terminal domain of LIP5 to increase our chances of success. But what would have

been different if we used the full-length protein? We probably would not observe the sandwich arrangement of double particles as the N-terminal domain would possibly have less space to oligomerize. Since the linker connecting the two domains in LIP5 is disordered, it is possible that we would not be able to see any additional part of that in the final map. On the other hand, we would be sure that the binding of the N-terminal domain to AQP2 resembles the real complexation as much as possible.

The only other available structure of an aquaporin in complex with another protein is the 25 Å model of the AQP0-CaM complex [76]. Both this and our complex share the same stoichiometry of two regulatory proteins binding diagonally to one aquaporin tetramer. However, for AQP0-CaM, each molecule of CaM is thought to bind two AQP0 C-terminal helices from neighbouring monomers while this is something that the resolution of our AQP2-LIP5 map does not allow us to draw any conclusions of.

Story 2: AQP5-PIP

In Paper IV, we have confirmed the previously suggested direct interaction between AQP5 and PIP using a co-elution assay and MST. The binding appears to be highly cooperative. Studying the binding affinities of truncated constructs, we have identified the distal C-terminus of AQP5 to be the binding site for PIP, not the C-terminal helix as it often is in other aquaporins. But where is the binding site on PIP located? Although PIP was found to bind to an extensive number of targets, the structural information about these interactions is limited. From the only crystal structure of PIP, in complex with zinc-α-glycoprotein (ZAG) [60], two binding sites on PIP were identified. The main one involves one of the β-strands which creates an antiparallel alignment with a neighbouring β-strand from ZAG. Such binding mode is unlikely in AQP5. It is much more probable that some of the loops of PIP are engaged in the interaction, like the residues on loops 4 and 6 which create the second binding site for ZAG. The only other binding affinity measured for PIP is for the binding to CD4 receptor where the K_D was 6 nM. That is about 100-fold stronger binding than what we have measured for PIP-AQP5 (570 ± 120 nM). This is not so surprising since CD4 also consists of β-sheets.

Our stoichiometry results show that likely only one molecule of PIP binds to one AQP5 tetramer. The obvious question is why is that. Based on our results, after the first PIP binds the three remaining C-termini of the tetramer are not available for interaction with a second molecule of PIP. Because of the flexibility of the distal termini the argument of steric clashes is most likely not founded. Either, for some reason, in our hands the interaction does not happen at the physiological scale or the

C-termini are all interacting with the same molecule of PIP. The latter is supported by the high level of cooperativity in the binding. Another plausible explanation could involve the phosphorylation site at Thr 259 of AQP5 which is part of the region where the binding site lies. Phosphorylation at this residue could prevent or be necessary for the interaction with PIP to happen and this should be further investigated.

Based on the relatively low affinity and the propensity of PIP to bind to a myriad of other proteins this interaction is likely to be very transient. Although the function of the complex is currently not known, it is possible that the binding happens during vesicle trafficking or microtubule binding since PIP is known to bind actin [56] and since in Sjögren's syndrome the trafficking of AQP5 is impaired [45]. G-actin binding is an important event in AQP2 exocytosis [122] and it could play a role in trafficking of AQP5 as well.

Story 3: AQP0-CaM

In Paper V we have confirmed that in liposomes the direct binding of CaM to AQP0 closes the channel, which was previously only tested in oocytes [14]. None of the three constructed phosphomimicking mutants could be closed by CaM, we therefore expected that none of those would bind to it. Interestingly, S231D is still able to bind CaM, though the binding mode is probably different. This is further supported by our MST results where the binding curve has an opposite direction than for the wild-type. When the binding was tested with phosphorylated peptides (as oppose to full-length proteins) the S231 phosphorylated peptide did not bind AQP0. This suggests that other parts of the protein also play a role in the binding, possibly the distal C-terminus, as in AQP2 binding to LIP5, or the loop D, as suggested by molecular simulations [123]. Contrarily to our results, these simulations observed an alternative binding mode for AQP0 phosphorylated at S229 and S235 [123]. Physiological relevance of such alternative binding remains to be elucidated.

S235 is the main phosphorylation site in human AQP0 and it gets increasingly more phosphorylated towards the inner part of the inner cortex of the lens [124]. Since based on our results S235D loses its Ca^{2+}/CaM sensitivity, this would mean that the regulation of channel gating by CaM is also decreased by lens maturation. However, in oocytes S235D retained its Ca^{2+} sensitivity, although the mechanism and the involvement of CaM are not clear. Moreover, the phosphorylation of S235 by protein kinase C is important for trafficking of AQP0 to the apical membrane after synthesis [78] and it is possible that, when studied in oocytes, some of the observed effects might in fact be due to AQP0 trafficking, rather than gating.

Concluding remarks and outlook

In this thesis I have described our studies of the regulation of three human isoforms of aquaporins – AQP0, AQP2 and AQP5. As a reader might have noticed the level of detail at which we have studied the three different isoforms is not the same. Much is already known about the regulation of AQP2 trafficking by phosphorylation and here we have contributed by a further knowledge of how this phosphorylation affects the binding of LIP5 and by further structural details of this complex. On the other side of the spectrum, not much is known about how PIP regulates the trafficking of AQP5. We have contributed with characterizing this interaction but the story still has a lot of loose ends. For example, since PIP is a secreted protein, it still remains unclear at which point does this interaction happen and why it needs to happen. I will be very curious to follow the research in this particular field in the future.

This thesis is a proof of how important posttranslational modifications are in regulating protein function. In the future, I expect that characterization of PTMs and their effect on function will be a subject of many more studies in many more protein systems.

We probed the effect of phosphorylation on the binding affinity of AQP2 to LIP5 and AQP0 to CaM. Similarly, in the future this effect should also be tested on AQP5 and its binding to PIP as AQP5 contains one phosphorylation site within the expected binding site as well as other phosphorylation sites outside of it. We also know that difference in the glycan chain on PIP affects the binding affinity towards CD4. It would be interesting to see whether this could be true for the interaction with AQP5 as well. During my time as a PhD student I have tried to express and purify a N77A mutant of PIP where the glycosylation site was mutated. The idea was to test whether the binding affinity for this mutant is any different from the wild type. However, this mutant repeatedly failed to purify, maybe because of the possible stabilizing effect of the glycosylation, and after many trials we have dropped the efforts.

The cell is a crowded environment, while all studies included in this thesis are done *in vitro*. These studies are necessary to understand the small, especially structural, details of proteins. However, further *in vivo* experiments will be needed to set the findings originating from this thesis into the context of the complex cellular organization.

I believe that the largest contribution of this thesis is the cryo-EM structure of AQP2 in complex with LIP5. Even though the resolution does not allow us to distinguish the atomic details of the complex, the method described in Paper III still provides a stepping stone, enabling and encouraging further studies of aquaporin complexes. I like to think that a higher resolution structure is just a few trials away and that only minor tweaks in sample preparation would get us there. The system of lipid nanodiscs seem to be very suitable for studying membrane proteins in cryo-EM. Since the protocol for reconstitution is quite optimized, I believe it could be easily applied onto other aquaporins in complexes with their regulatory proteins and I hope to see many beautiful cryo-EM structures of these in the future.

References

[1] Hartley, H. Origin of the Word 'Protein'. *Nature*. **1951**, p 244, https://doi.org/10.1038/168244a0.

[2] Lodish, H.; Berk, A.; Zipursky, S. *Molecular Cell Biology*, 4th ed.; W.H. Freeman: New York, **2000**.

[3] Kitchen, P.; Day, R. E.; Salman, M. M.; Conner, M. T.; Bill, R. M.; Conner, A. C. Beyond Water Homeostasis : Diverse Functional Roles of Mammalian Aquaporins. *BBA - Gen. Subj.* **2015**, *1850*, 2410–2421, https://doi.org/10.1016/j.bbagen.2015.08.023.

[4] Verkman, A. S. Aquaporins in Clinical Medicine. *Annu. Rev. Med.* **2012**, *23* (63), 303–316, https://doi.org/10.1146/annurev-med-043010-193843.

[5] Murata, K.; Mitsuoka, K.; Hirai, T.; Walz, T.; Agre, P.; Heymann, J. B.; Engel, A.; Fujiyoshi, Y. Structural Determinants of Water Permeation through Aquaporin-1. *Nature* **2000**, *407*, 599–605.

[6] Eriksson, U. K.; Fischer, G.; Friemann, R.; Enkavi, G.; Tajkhorshid, E.; Neutze, R. Subangstrom Resolution X-Ray Structure Details Aquaporin-Water Interactions. *Science (80-.).* **2013**, *340* (6138), 1346–1349, https://doi.org/10.1126/science.1234306.

[7] Kreida, S.; Törnroth-Horsefield, S. Structural Insights into Aquaporin Selectivity and Regulation. *Curr. Opin. Struct. Biol.* **2015**, No. 33, 126–134, https://doi.org/10.1016/j.sbi.2015.08.004.

[8] Roche, J. V.; Törnroth-Horsefield, S. Aquaporin Protein-Protein Interactions. *Int. J. Mol. Sci.* **2017**, *18*, 2255, https://doi.org/10.3390/ijms18112255.

[9] Nesverova, V.; Törnroth-horsefield, S. Phosphorylation-Dependent Regulation of Mammalian Aquaporins. *Cells* **2019**, *8* (82), https://doi.org/10.3390/cells8020082.

[10] Frick, A.; Eriksson, U. K.; de Mattia, F.; Oberg, F.; Hedfalk, K.; Neutze, R.; de Grip, W. J.; Deen, P. M. T.; Tornroth-Horsefield, S. X-Ray Structure of Human Aquaporin 2 and Its Implications for Nephrogenic Diabetes Insipidus and Trafficking. *Proc. Natl. Acad. Sci.* **2014**, *111* (17), 6305–6310, https://doi.org/10.1073/pnas.1321406111.

[11] Törnroth-Horsefield, S.; Wang, Y.; Hedfalk, K.; Johanson, U.; Karlsson, M.; Tajkhorshid, E.; Neutze, R.; Kjellbom, P. Structural Mechanism of Plant Aquaporin Gating. *Nature* **2006**, *439* (7077), 688–694, https://doi.org/10.1038/nature04316.

[12] Tran, T. L.; Hamann, S.; Heegaard, S. Aquaporins in the Eye. In *Aquaporins. Advances in Experimental Medicine and Biology*; Sprenger: Dordrecht, **2017**; Vol. 969, https://doi.org/10.1007/978-94-024-1057-0.
[13] Girsch, S. J.; Peracchia, C. Lens Cell-to-Cell Channel Protein: I. Self-Assembly into Liposomes and Permeability Regulation by Calmodulin. *J. Membr. Biol.* **1985**, *83* (3), 217–225, https://doi.org/10.1007/BF01868696.
[14] Kalman, K.; Németh-Cahalan, K. L.; Froger, A.; Hall, J. E. Phosphorylation Determines the Calmodulin-Mediated Ca2+response and Water Permeability of AQP0. *J. Biol. Chem.* **2008**, *283* (30), 21278–21283, https://doi.org/10.1074/jbc.M801740200.
[15] Gunnarson, E.; Zelenina, M.; Axehult, G.; Song, Y.; Bondar, A.; Krieger, P.; Brismar, H.; Zelenin, S.; Aperia, A. Identification of a Molecular Target for Glutamate Regulation of Astrocyte Water Permeability. *Glia* **2008**, *56* (6), 587–596, https://doi.org/10.1002/glia.20627.
[16] Janosi, L.; Ceccarelli, M. The Gating Mechanism of the Human Aquaporin 5 Revealed by Molecular Dynamics Simulations. *PLoS One* **2013**, *8*, e59897, https://doi.org/10.1371/journal.pone.0059897.
[17] Rodrigues, C.; Mósca, A. F.; Martins, A. P.; Nobre, T.; Prista, C.; Antunes, F.; Gasparovic, A. C.; Soveral, G. Rat Aquaporin-5 Is PH-Gated Induced by Phosphorylation and Is Implicated in Oxidative Stress. *Int. J. Mol. Sci.* **2016**, *17* (12), https://doi.org/10.3390/ijms17122090.
[18] Gotfryd, K.; Mósca, A. F.; Missel, J. W.; Truelsen, S. F.; Wang, K.; Spulber, M.; Krabbe, S.; Hélix-nielsen, C.; Laforenza, U.; Soveral, G.; et al. Human Adipose Glycerol Flux Is Regulated by a PH Gate in AQP10. *Nat. Commun.* **2018**, *9* (4749), https://doi.org/10.1038/s41467-018-07176-z.
[19] Conner, A. C.; Bill, R. M.; Conner, M. T. An Emerging Consensus on Aquaporin Translocation as a Regulatory Mechanism. *Mol. Membr. Biol.* **2013**, *30* (1), 101–112, https://doi.org/10.3109/09687688.2012.743194.
[20] Conner, M. T.; Conner, A. C.; Brown, J. E. P.; Bill, R. M. Membrane Trafficking of Aquaporin 1 Is Mediated by Protein Kinase C via Microtubules and Regulated by Tonicity. *Biochemistry* **2010**, *49* (5), 821–823, https://doi.org/10.1021/bi902068b.
[21] Johnson, M.; Zaretskaya, I.; Raytselis, Y.; Merezhuk, Y.; McGinnis, S.; Madden, T. L. NCBI BLAST: A Better Web Interface. *Nucleic Acids Res.* **2008**, *36* (Web Server issue), W5–W9, https://doi.org/10.1093/nar/gkn201.
[22] Kitchen, P.; Öberg, F.; Sjöhamn, J.; Hedfalk, K.; Bill, R. M.; Conner, A. C.; Conner, M. T.; Törnroth-Horsefield, S. Plasma Membrane Abundance of Human Aquaporin 5 Is Dynamically Regulated by Multiple Pathways. *PLoS One* **2015**, *10* (11), 1–17, https://doi.org/10.1371/journal.pone.0143027.

[23] Matsuzaki, T.; Yaguchi, T.; Shimizu, K.; Kita, A.; Ishibashi, K.; Takata, K. The Distribution and Function of Aquaporins in the Kidney: Resolved and Unresolved Questions. *Anat. Sci. Int.* **2017**, *92* (2), 187–199, https://doi.org/10.1007/s12565-016-0325-2.
[24] King, L. S.; Kozono, D.; Agre, P. From Structure to Disease: The Evolving Tale of Aquaporin Biology. *Nat. Rev. Mol. Cell Biol.* **2004**, *5* (9), 687–698, https://doi.org/10.1038/nrm1469.
[25] Nejsum, L. N. The Renal Plumbing System: Aquaporin Water Channels. *Cell. Mol. Life Sci.* **2005**, *62* (15), 1692–1706, https://doi.org/10.1007/s00018-005-4549-x.
[26] Calvanese, L.; D'Auria, G.; Vangone, A.; Falcigno, L.; Oliva, R. Structural Basis for Mutations of Human Aquaporins Associated to Genetic Diseases. *Int. J. Mol. Sci.* **2018**, *19* (6), https://doi.org/10.3390/ijms19061577.
[27] Kuwahara, M.; Fushimi, K.; Terada, Y.; Bai, L.; Marumo, F.; Sasaki, S. CAMP-Dependent Phosphorylation Stimulates Water Permeability of Aquaporin-Collecting Duct Water Channel Protein Expressed in Xenopus Oocytes. *J. Biol. Chem.* **1995**, *270* (18), 10384–10387.
[28] Kamsteeg, E.-J.; Hendriks, G.; Boone, M.; Konings, I. B. M.; Oorschot, V.; van der Sluijs, P.; Klumperman, J.; Deen, P. M. T. Short-Chain Ubiquitination Mediates the Regulated Endocytosis of the Aquaporin-2 Water Channel. *Proc. Natl. Acad. Sci.* **2006**, *103* (48), 18344–18349, https://doi.org/10.1073/pnas.0604073103.
[29] Van Balkom, B. W. M.; Savelkoul, P. J. M.; Markovich, D.; Hofman, E.; Nielsen, S.; Van Der Sluijs, P.; Deen, P. M. T. The Role of Putative Phosphorylation Sites in the Targeting and Shuttling of the Aquaporin-2 Water Channel. *J. Biol. Chem.* **2002**, *277* (44), 41473–41479, https://doi.org/10.1074/jbc.M207525200.
[30] Brown, D.; Hasler, U.; Nunes, P.; Bouley, R.; Lu, H. A. J. Phosphorylation Events and the Modulation of Aquaporin 2 Cell Surface Expression. *Curr. Opin. Nephrol. Hypertens.* **2008**, *17* (5), 491–498, https://doi.org/10.1097/MNH.0b013e3283094eb1.
[31] Hoffert, J. D.; Fenton, R. A.; Moeller, H. B.; Simons, B.; Tchapyjnikov, D.; McDill, B. W.; Yu, M. J.; Pisitkun, T.; Chen, F.; Knepper, M. A. Vasopressin-Stimulated Increase in Phosphorylation at Ser269 Potentiates Plasma Membrane Retention of Aquaporin-2. *J. Biol. Chem.* **2008**, *283* (36), 24617–24627, https://doi.org/10.1074/jbc.M803074200.
[32] Tamma, G.; Robben, J. H.; Trimpert, C.; Boone, M.; Deen, P. M. T. Regulation of AQP2 Localization by S256 and S261 Phosphorylation and Ubiquitination. *AJP Cell Physiol.* **2011**, *300* (3), C636–C646, https://doi.org/10.1152/ajpcell.00433.2009.
[33] Fenton, R. a; Moeller, H. B.; Hoffert, J. D.; Yu, M.-J.; Nielsen, S.; Knepper, M. a. Acute Regulation of Aquaporin-2 Phosphorylation at Ser-264 by Vasopressin. *Proc Natl Acad Sci U S A* **2008**, *105* (8), 3134–3139, https://doi.org/10.1073/pnas.0712338105.

[34] Trimpert, C.; Wesche, D.; De Groot, T.; Pimentel Rodriguez, M. M.; Wong, V.; Van Den Berg, D. T. M.; Cheval, L.; Ariza, C. A.; Doucet, A.; Stagljar, I.; et al. NDFIP Allows NEDD4/NEDD4L-Induced AQP2 Ubiquitination and Degradation. *PLoS One* **2017**, *12* (9), 1–18, https://doi.org/10.1371/journal.pone.0183774.
[35] Roche, J. V.; Nesverova, V.; Olsson, C.; Deen, P. M. T.; Törnroth-Horsefield, S. Structural Insights into AQP2 Targeting to Multivesicular Bodies. *Int. J. Mol. Sci.* **2019**, *20* (5351), 1–16, https://doi.org/10.3390/ijms20215351.
[36] Schmidt, O.; Teis, D. The ESCRT Machinery. *Curr. Biol.* **2012**, *22* (4), R116–R120, https://doi.org/10.1016/j.cub.2012.01.028.
[37] Xiao, J.; Xia, H.; Zhou, J.; Azmi, I.; Davies, B. .; Katzmann, D. J.; Xu, Z. Structural Basis of Vta1 Function in the Multi-Vesicular Body Sorting Pathway. *Dev. Cell* **2008**, *14* (1), 37–49, https://doi.org/10.1016/j.devcel.2007.10.013.Structural.
[38] Azmi, I.; Davies, B.; Dimaano, C.; Payne, J.; Eckert, D.; Babst, M.; Katzmann, D. J. Recycling of ESCRTs by the AAA-ATPase Vps4 Is Regulated by a Conserved VSL Region in Vta 1. *J. Cell Biol.* **2006**, *172* (5), 705–717, https://doi.org/10.1083/jcb.200508166.
[39] Shim, S.; Merrill, S. A.; Hanson, P. I. Novel Interactions of ESCRT-III with LIP5 and VPS4 and Their Implications for ESCRT-III Disassembly. *Mol. Biol. Cell* **2008**, *19* (6), 2661–2672, https://doi.org/10.1091/mbc.e07-12-1263.
[40] Vild, C. J.; Li, Y.; Guo, E. Z.; Liu, Y.; Xu, Z. A Novel Mechanism of Regulating the ATPase VPS4 by Its Cofactor LIP5 and the Endosomal Sorting Complex Required for Transport (ESCRT)-III Protein CHMP5. *J. Biol. Chem.* **2015**, *290* (11), 7291–7303, https://doi.org/10.1074/jbc.M114.616730.
[41] Van Balkom, B. W. M.; Boone, M.; Hendriks, G.; Kamsteeg, E. J.; Robben, J. H.; Stronks, H. C.; Van Der Voorde, A.; Van Herp, F.; Van Der Sluijs, P.; Deen, P. M. T. LIP5 Interacts with Aquaporin 2 and Facilitates Its Lysosomal Degradation. *J. Am. Soc. Nephrol.* **2009**, *20* (5), 990–1001, https://doi.org/10.1681/ASN.2008060648.
[42] Guo, E. Z.; Xu, Z. Distinct Mechanisms of Recognizing Endosomal Sorting Complex Required for Transport III (ESCRT-III) Protein IST1 by Different Microtubule Interacting and Trafficking (MIT) Domains. *J. Biol. Chem.* **2015**, *290* (13), 8396–8408, https://doi.org/10.1074/jbc.M114.607903.
[43] Raina, S.; Preston, G. M.; Guggino, W. B.; Agre, P. Molecular Cloning and Characterization of an Aquaporin CDNA from Salivary, Lacrimal and Respiratory Tissues. *J. Biol. Chem.* **1995**, *270* (4), 1908–1912.
[44] Steinfeld, S.; Cogan, E.; King, L. S.; Agre, P.; Kiss, R.; Delporte, C. Abnormal Distribution of Aquaporin-5 Water Channel Protein in Salivary Glands from Sjögren's Syndrome Patients. *Lab. Investig.* **2001**, *81* (2), 143–148, https://doi.org/10.1038/labinvest.3780221.

[45] Tsubota, K.; Hirai, S.; King, L.; Agre, P.; Ishida, N. Defective Cellular Trafficking of Lacrimal Gland Aquaporin-5 in Sjögren's Syndrome. *Lancet* **2001**, *357*, 688–689.
[46] Lee, B. H.; Gauna, A. E.; Perez, G.; Park, Y.; Pauley, K. M.; Kawai, T.; Cha, S. Autoantibodies against Muscarinic Type 3 Receptor in Sjögren's Syndrome Inhibit Aquaporin 5 Trafficking. *PLoS One* **2013**, *8* (1), e53113, https://doi.org/10.1371/journal.pone.0053113.
[47] Sisto, M.; Lorusso, L.; Ingravallo, G.; Nico, B.; Ribatti, D.; Ruggieri, S.; Lofrumento, D. D.; Lisi, S. Abnormal Distribution of AQP4 in Minor Salivary Glands of Primary Sjögren's Syndrome Patients. *Autoimmunity* **2017**, *50* (4), 202–210, https://doi.org/10.1080/08916934.2017.1341495.
[48] Alam, J.; Choi, Y. S.; Koh, J. H.; Kwok, S.-K.; Park, S.-H.; Song, Y. W.; Park, K.; Choi, Y. Detection of Autoantibodies against Aquaporin-1 in the Sera of Patients with Primary Sjögren's Syndrome. *Immune Netw.* **2017**, *17* (2), 103–109, https://doi.org/10.4110/in.2017.17.2.103.
[49] Mostafa, S.; Seamon, V.; Azzarolo, A. M. Influence of Sex Hormones and Genetic Predisposition in Sjögren's Syndrome: A New Clue to the Immunopathogenesis of Dry Eye Disease. *Exp. Eye Res.* **2012**, *96* (1), 88–97, https://doi.org/10.1016/j.exer.2011.12.016.
[50] Alam, J.; Koh, J. H.; Kim, N.; Kwok, S.-K.; Park, S.-H.; Song, Y. W.; Park, K.; Choi, Y. Autoantibodies against Aquaporin-5, a Novel Biomarker of Primary Sjögren's Syndrome. *Meta Gene* **2018**, *17*, S14, https://doi.org/10.1016/J.MGENE.2018.05.057.
[51] Ohashi, Y.; Tsuzaka, K.; Takeuchi, T.; Sasaki, Y.; Tsubota, K. Altered Distribution of Aquaporin 5 and Its C-Terminal Binding Protein in the Lacrimal Glands of a Mouse Model for Sjögren's Syndrome. *Curr. Eye Res.* **2008**, *33* (8), 621–629, https://doi.org/10.1080/02713680802262819.
[52] Zhou, L.; Wei, R.; Zhao, P.; Koh, S. K.; Beuerman, R. W.; Ding, C. Proteomic Analysis Revealed the Altered Tear Protein Profile in a Rabbit Model of Sjögren's Syndrome-Associated Dry Eye. *Proteomics* **2013**, *13* (16), 2469–2481, https://doi.org/10.1002/pmic.201200230.
[53] Gallo, A.; Martini, D.; Sernissi, F.; Giacomelli, C.; Pepe, P.; Rossi, C.; Riveros, P.; Mosca, M.; Alevizos, I.; Baldini, C. Gross Cystic Disease Fluid Protein-15(GCDFP-15)/Prolactin-Inducible Protein (PIP) as Functional Salivary Biomarker for Primary Sjögren's Syndrome. *J. Genet. Syndr. Gene Ther.* **2013**, *04* (04), https://doi.org/10.4172/2157-7412.1000140.
[54] Shiu, R. P. C.; Iwasiow, B. M. Prolactin-Inducible Proteins in Human Breast Cancer Cells. *J. Biol. Chem.* **1985**, *260* (20), 11307–11313.
[55] Vandewalle, B.; Hornez, L.; Vennin, P.; Peyrat, J. P.; Lefebvre, J. Further Characterization of the Light Breast Cyst Fluid Protein, GCDFP-15. *Biochimie* **1986**, *68*, 649–656, https://doi.org/10.1016/S0300-9084(86)80159-6.
[56] Akiyama, K.; Kimura, H. Isolation of a New Actin-Binding Protein from Human Seminal Plasma. *Biochim. Biophys. Acta* **1990**, *1040* (2), 206–210, https://doi.org/10.1016/0167-4838(90)90077-S.

[57] Schenkels, L. C. P. M.; Ligtenberg, A. J. M.; Veerman, E. C. I.; Van Nieum Amerongen, A. Interaction of the Salivary Glycoprotein EP-GP with the Bacterium Streptococcus Salivarius HB. *J. Dent. Res.* **1993**, *72* (12), 1559–1565, https://doi.org/10.1177/00220345930720120501.

[58] Autiero, M.; Cammarota, G.; Friedlein, a; Zulauf, M.; Chiappetta, G.; Dragone, V.; Guardiola, J. A 17-KDa CD4-Binding Glycoprotein Present in Human Seminal Plasma and in Breast Tumor Cells. *Eur. J. Immunol.* **1995**, *25* (5), 1461–1464, https://doi.org/10.1002/eji.1830250550.

[59] Hassan, M. I.; Waheed, a; Yadav, S.; Singh, T. P.; Ahmad, F. Prolactin Inducible Protein in Cancer, Fertility and Immunoregulation: Structure, Function and Its Clinical Implications. *Cell. Mol. Life Sci.* **2009**, *66* (3), 447–459, https://doi.org/10.1007/s00018-008-8463-x.

[60] Hassan, M. I.; Bilgrami, S.; Kumar, V.; Singh, N.; Yadav, S.; Kaur, P.; Singh, T. P. Crystal Structure of the Novel Complex Formed between Zinc Alpha2-Glycoprotein (ZAG) and Prolactin-Inducible Protein (PIP) from Human Seminal Plasma. *J. Mol. Biol.* **2008**, *384* (3), 663–672, https://doi.org/10.1016/j.jmb.2008.09.072.

[61] Osawa, M.; Seto, Y.; Yukawa, N.; Saito, T.; Takeichi, S. A 20-KDa Protein in Human Seminal Plasma That Is Identical to Gross Cystic Disease Fluid Protein 15 and Prolactin-Inducible Protein. *Arch. Androl.* **1996**, *36* (1), 29–39.

[62] Autiero, M.; Gaubin, M.; Mani, J. C.; Castejon, C.; Martin, M.; El Marhomy, S.; Guardiola, J.; Piatier-Tonneau, D. Surface Plasmon Resonance Analysis of Gp17, a Natural CD4 Ligand from Human Seminal Plasma Inhibiting Human Immunodeficiency Virus Type-1 Gp120-Mediated Syncytium Formation. *Eur. J. Biochem.* **1997**, *245* (1), 208–213, https://doi.org/10.1111/j.1432-1033.1997.00208.x.

[63] Kumar, S.; Tomar, A. K.; Singh, S.; Saraswat, M.; Singh, S.; Singh, T. P.; Yadav, S. Human Serum Albumin as a New Interacting Partner of Prolactin Inducible Protein in Human Seminal Plasma. *Int. J. Biol. Macromol.* **2012**, *50* (2), 317–322, https://doi.org/10.1016/j.ijbiomac.2011.12.015.

[64] Chiu, W. W. C.; Chamley, L. W. Human Seminal Plasma Prolactin-Inducible Protein Is an Immunoglobulin G-Binding Protein. *J. Reprod. Immunol.* **2003**, *60*, 97–111, https://doi.org/10.1016/S0165-0378(03)00084-6.

[65] Hassan, M. I.; Kumar, V.; Singh, T. P.; Yadav, S. Purification and Characterization of Zinc Alpha2-Glycoprotein-Prolactin Inducible Protein Complex from Human Seminal Plasma. *J. Sep. Sci.* **2008**, *31*, 2318–2324.

[66] Dunia, I.; Manenti, S.; Rousselet, A.; Benedetti, E. L. Electron Microscopic Observations of Reconstituted Proteoliposomes with the Purified Major Intrinsic Membrane Protein of Eye Lens Fibers. *J. Cell Biol.* **1987**, *105*, 1679–1689, https://doi.org/10.1083/jcb.105.4.1679.

[67] Verkman, a. S. Role of Aquaporin Water Channels in Eye Function. *Exp. Eye Res.* **2003**, *76* (2), 137–143, https://doi.org/10.1016/S0014-4835(02)00303-2.
[68] Engel, A.; Fujiyoshi, Y.; Gonen, T.; Walz, T. Junction-Forming Aquaporins. *Curr. Opin. Struct. Biol.* **2008**, *18* (2), 229–235, https://doi.org/10.1016/j.sbi.2007.11.003.
[69] Gonen, T.; Sliz, P.; Kistler, J.; Cheng, Y.; Walz, T. Aquaporin-0 Membrane Junctions Reveal the Structure of a Closed Water Pore. *Nature* **2004**, *429*, 193–197.
[70] Gonen, T.; Cheng, Y.; Sliz, P.; Hiroaki, Y.; Fujiyoshi, Y.; Harrison, S. C.; Walz, T. Lipid-Protein Interactions in Double-Layered Two-Dimensional AQP0 Crystals. *Nature* **2005**, *438* (7068), 633–638, https://doi.org/10.1038/nature04321.
[71] Németh-Cahalan, K. L.; Hall, J. E. PH and Calcium Regulate the Water Permeability of Aquaporin 0. *J. Biol. Chem.* **2000**, *275* (10), 6777–6782, https://doi.org/10.1074/jbc.275.10.6777.
[72] Hoeflich, K. P.; Ikura, M. Calmodulin in Action: Diversity in Target Recognition and Activation Mechanisms. *Cell* **2002**, *108* (6), 739–742, https://doi.org/10.1016/S0092-8674(02)00682-7.
[73] J. Girsch, S.; Peracchia, C. Calmodulin Interacts with a C-Terminus Peptide from the Lens Membrane Protein MIP26. *Curr. Eye Res.* **1991**, *10* (9), 839–849.
[74] Reichow, S. L.; Gonen, T. Noncanonical Binding of Calmodulin to Aquaporin-0: Implications for Channel Regulation. *Structure* **2008**, *16* (9), 1389–1398, https://doi.org/10.1016/j.str.2008.06.011.
[75] Reichow, S. L.; Clemens, D. M.; Freites, J. A.; Németh-cahalan, K. L. Allosteric Mechanism of Water Channel Gating by Ca2+–Calmodulin. *Nat Struct Mol Biol* **2013**, *20* (9), 1085–1092, https://doi.org/10.1038/nsmb.2630.Allosteric.
[76] Reichow, S. L.; Clemens, D. M.; Freites, J. A.; Németh-Cahalan, K. L.; Heyden, M.; Tobias, D. J.; Hall, J. E.; Gonen, T. Allosteric Mechanism of Water-Channel Gating by Ca 2+ -Calmodulin. *Nat. Struct. Mol. Biol.* **2013**, *20* (9), 1085–1092, https://doi.org/10.1038/nsmb.2630.
[77] Lindsey Rose, K. M.; Wang, Z.; Magrath, G. N.; Hazard, E. S.; Hildebrandt, J. D.; Schey, K. L. Aquaporin 0-Calmodulin Interaction and the Effect of Aquaporin 0 Phosphorylation. *Biochemistry* **2008**, *47* (1), 339–347, https://doi.org/10.1021/bi701980t.
[78] Golestaneh, N.; Fan, J.; Zelenka, P.; Chepelinsky, A. B. PKC Putative Phosphorylation Site Ser235 Is Required for MIP/AQP0 Translocation to the Plasma Membrane. *Mol. Vis.* **2008**, *14* (May), 1006–1014.
[79] Tseng, W. C.; Lin, J. W.; Wei, T. Y.; Fang, T. Y. A Novel Megaprimed and Ligase-Free, PCR-Based, Site-Directed Mutagenesis Method. *Anal. Biochem.* **2008**, *375* (2), 376–378, https://doi.org/10.1016/j.ab.2007.12.013.

[80] Eckart, M. R.; Bussineau, C. M. Quality and Authenticity of Heterologous Proteins Synthesized in Yeast. *Curr. Opin. Biotechnol.* **1996**, *7* (5), 525–530, https://doi.org/10.1016/S0958-1669(96)80056-5.
[81] Öberg, F.; Ekvall, M.; Nyblom, M.; Backmark, A.; Neutze, R.; Hedfalk, K. Insight into Factors Directing High Production of Eukaryotic Membrane Proteins; Production of 13 Human AQPs in Pichia Pastoris. *Mol. Membr. Biol.* **2009**, *26* (4), 215–227, https://doi.org/10.1080/09687680902862085.
[82] Horsefield, R.; Nordén, K.; Fellert, M.; Backmark, A.; Törnroth-Horsefield, S.; Terwisscha van Scheltinga, A. C.; Kvassman, J.; Kjellbom, P.; Johanson, U.; Neutze, R. High-Resolution x-Ray Structure of Human Aquaporin 5. *Proc. Natl. Acad. Sci. U. S. A.* **2008**, *105* (36), 13327–13332, https://doi.org/10.1073/pnas.0801466105.
[83] Frick, A.; Järvå, M.; Törnroth-Horsefield, S. Structural Basis for PH Gating of Plant Aquaporins. *FEBS Lett.* **2013**, *587* (7), 989–993, https://doi.org/10.1016/j.febslet.2013.02.038.
[84] Macauley-Patrick, S.; Fazenda, M. L.; McNeil, B.; Harvey, L. M. Heterologous Protein Production Using the Pichia Pastoris Expression System. *Yeast* **2005**, *22* (4), 249–270, https://doi.org/10.1002/yea.1208.
[85] Kinoshita, E.; Kinoshita-Kikuta, E.; Sugiyama, Y.; Fukada, Y.; Ozeki, T.; Koike, T. Highly Sensitive Detection of Protein Phosphorylation by Using Improved Phos-Tag Biotin. *Proteomics* **2012**, *12* (7), 932–937, https://doi.org/10.1002/pmic.201100639.
[86] Kurizan; Konforti; Wemmer. Molecular Recognition : The Thermodynamics of Binding. In *The Molecules of Life*; Garland Publishing, **2009**.
[87] Schreiber, G.; Keating, A. E. Protein Binding Specificity versus Promiscuity. *Current Opinion in Structural Biology*. February **2011**, pp 50–61, https://doi.org/10.1016/j.sbi.2010.10.002.
[88] Jameson, D. M. *Introduction to Fluorescence*; Taylor & Francis, **2014**.
[89] Jerabek-Willemsen, M.; André, T.; Wanner, R.; Roth, H. M.; Duhr, S.; Baaske, P.; Breitsprecher, D. MicroScale Thermophoresis: Interaction Analysis and Beyond. *J. Mol. Struct.* **2014**, https://doi.org/10.1016/j.molstruc.2014.03.009.
[90] Duhr, S.; Braun, D. Why Molecules Move along a Temperature Gradient. *Proc. Natl. Acad. Sci. U. S. A.* **2006**, *103* (52), 19678–19682, https://doi.org/10.1073/pnas.0603873103.
[91] Wu, Y.; Li, Q.; Chen, X. Z. Detecting Protein-Protein Interactions by Far Western Blotting. *Nat. Protoc.* **2007**, *2* (12), 3278–3284, https://doi.org/10.1038/nprot.2007.459.
[92] Bayburt, T. H.; Grinkova, Y. V; Sligar, S. G. Self-Assembly of Discoidal Phospholipid Bilayer Nanoparticles with Membrane Scaffold Proteins. **2002**, 1–4, https://doi.org/10.1021/nl025623k.

[93] Ritchie, T. K.; Grinkova, Y. V.; Bayburt, T. H.; Denisov, I. G.; Zolnerciks, J. K.; Atkins, W. M.; Sligar, S. G. Reconstitution of Membrane Proteins in Phospholipid Bilayer Nanodiscs. In *Methods in Enzymology*; Elsevier, **2009**; Vol. 464, pp 211–231, https://doi.org/10.1016/S0076-6879(09)64011-8.
[94] Efremov, G. R.; Gatsogiannis, C.; Raunser, S. *Lipid Nanodiscs as a Tool for High-Resolution Structure Determination of Membrane Proteins by Single-Particle*, 1st ed.; Elsevier Inc., **2017**; Vol. 594, https://doi.org/10.1016/bs.mie.2017.05.007.
[95] Kynde, S. A. R.; Skar-Gislinge, N.; Pedersen, M. C.; Midtgaard, S. R.; Simonsen, J. B.; Schweins, R.; Mortensen, K.; Arleth, L. Small-Angle Scattering Gives Direct Structural Information about a Membrane Protein inside a Lipid Environment. *Acta Crystallogr. Sect. D Biol. Crystallogr.* **2014**, *70* (2), 371–383, https://doi.org/10.1107/S1399004713028344.
[96] Murakami, T. Phospholipid Nanodisc Engineering for Drug Delivery Systems. *Biotechnol. J.* **2012**, *7* (6), 762–767, https://doi.org/10.1002/biot.201100508.
[97] Rupp, B. *Biomolecular Crystallography*; Garland Science, **2010**.
[98] Egelman, E. H. The Current Revolution in Cryo-EM. *Biophysical Journal*. Biophysical Society 2016, pp 1008–1012, https://doi.org/10.1016/j.bpj.2016.02.001.
[99] Vinothkumar, K. R. Membrane Protein Structures without Crystals, by Single Particle Electron Cryomicroscopy. *Curr. Opin. Struct. Biol.* **2015**, *33*, 103–114, https://doi.org/10.1016/j.sbi.2015.07.009.
[100] Cachau, R. E.; Zhu, J.; Nicklaus, M. C. The Upcoming Subatomic Resolution Revolution. *Curr. Opin. Struct. Biol.* **2019**, *58*, 53–58, https://doi.org/10.1016/j.sbi.2019.05.013.
[101] Dubochet, J.; McDowall, A. W. Vitrification of Pure Water for Electron Microscopy. *J. Microsc.* **1981**, *124* (3), 3–4, https://doi.org/10.1111/j.1365-2818.1981.tb02483.x.
[102] Thompson, R. F.; Walker, M.; Siebert, C. A.; Muench, S. P.; Ranson, N. A. An Introduction to Sample Preparation and Imaging by Cryo-Electron Microscopy for Structural Biology. *Methods* **2016**, *100*, 3–15, https://doi.org/10.1016/j.ymeth.2016.02.017.
[103] Cheng, Y.; Grigorieff, N.; Penczek, P. A.; Walz, T. A Primer to Single-Particle Cryo-Electron Microscopy. *Cell* **2015**, *161* (3), 438–449, https://doi.org/10.1016/j.cell.2015.03.050.
[104] Hauer, F.; Gerle, C.; Fischer, N.; Oshima, A.; Shinzawa-Itoh, K.; Shimada, S.; Yokoyama, K.; Fujiyoshi, Y.; Stark, H. GraDeR: Membrane Protein Complex Preparation for Single-Particle Cryo-EM. *Structure* **2015**, *23* (9), 1769–1775, https://doi.org/10.1016/j.str.2015.06.029.
[105] Cao, E.; Liao, M.; Cheng, Y.; Julius, D. TRPV1 Structures in Distinct Conformations Reveal Activation Mechanisms. *Nature* **2013**, *504* (7478), 113–118, https://doi.org/10.1038/nature12823.

[106] Parmar, M.; Rawson, S.; Scarff, C. A.; Goldman, A.; Dafforn, T. R.; Muench, S. P.; Postis, V. L. G. Using a SMALP Platform to Determine a Sub-Nm Single Particle Cryo-EM Membrane Protein Structure. *Biochimica et Biophysica Acta - Biomembranes*. **2018**, pp 378–383, https://doi.org/10.1016/j.bbamem.2017.10.005.
[107] Penczek, P. A. *Resolution Measures in Molecular Electron Microscopy*, 1st ed.; Elsevier Inc., **2010**; Vol. 482, https://doi.org/10.1016/S0076-6879(10)82003-8.
[108] Zi Tan, Y.; Baldwin, P. R.; Davis, J. H.; Williamson, J. R.; Potter, C. S.; Carragher, B.; Lyumkis, D. Addressing Preferred Specimen Orientation in Single-Particle Cryo-EMthrough Tilting. *Nat. Methods* **2017**, *14* (8), 793–796, https://doi.org/10.1038/nmeth.4347.
[109] Schey, K. L.; Little, M.; Fowler, J. G.; Crouch, R. K. Characterization of Human Lens Major Intrinsic Protein Structure. *Investig. Ophthalmol. Vis. Sci.* **2000**, *41* (1), 175–182.
[110] Kreida, S.; Roche, J. V.; Olsson, C.; Linse, S.; Törnroth-Horsefield, S. Protein–Protein Interactions in AQP Regulation – Biophysical Characterization of AQP0–CaM and AQP2–LIP5 Complex Formation. *Faraday Discuss.* **2018**, https://doi.org/10.1039/C8FD00065D.
[111] Azmi, I. F.; Davies, B. A.; Xiao, J.; Babst, M.; Xu, Z.; Katzmann, D. J. ESCRT-III Family Members Stimulate Vps4 ATPase Activity Directly or via Vta1. *Dev. Cell* **2008**, *14* (1), 50–61, https://doi.org/10.1016/j.devcel.2007.10.021.
[112] Roche, J. V.; Survery, S.; Kreida, S.; Nesverova, V.; Ampah-Korsah, H.; Gourdon, M.; Deen, P. M. T.; Törnroth-Horsefield, S. Phosphorylation of Human Aquaporin 2 (AQP2) Allosterically Controls Its Interaction with the Lysosomal Trafficking Protein LIP5. *J. Biol. Chem.* **2017**, *292* (35), 14636–14648, https://doi.org/10.1074/jbc.M117.788364.
[113] Van Zundert, G. C. P.; Rodrigues, J. P. G. L. M.; Trellet, M.; Schmitz, C.; Kastritis, P. L.; Karaca, E.; Melquiond, A. S. J.; Van Dijk, M.; De Vries, S. J.; Bonvin, A. M. J. J. The HADDOCK2.2 Web Server: User-Friendly Integrative Modeling of Biomolecular Complexes. *J. Mol. Biol.* **2016**, *428* (4), 720–725, https://doi.org/10.1016/j.jmb.2015.09.014.
[114] Pettersen, E. F.; Goddard, T. D.; Huang, C. C.; Couch, G. S.; Greenblatt, D. M.; Meng, E. C.; Ferrin, T. E. UCSF Chimera - A Visualization System for Exploratory Research and Analysis. *J. Comput. Chem.* **2004**, *25* (13), 1605–1612, https://doi.org/10.1002/jcc.20084.
[115] Caputo, E.; Autiero, M.; Mani, J. C.; Basmociogullari, S.; Piatier-Tonneau, D.; Guardiola, J. Differential Antibody Reactivity and CD4 Binding of the Mammary Tumor Marker Protein GCDFP-15 from Breast Cyst and Its Counterparts from Exocrine Epithelia. *Int. J. Cancer* **1998**, *78* (1), 76–85.
[116] Schaefer, J. V.; Plückthun, A. Engineering Aggregation Resistance in IgG by Two Independent Mechanisms: Lessons from Comparison of Pichia Pastoris and Mammalian Cell Expression. *J. Mol. Biol.* **2012**, *417* (4), 309–335, https://doi.org/10.1016/j.jmb.2012.01.027.

[117] Sjöhamn, J.; Hedfalk, K. Unraveling Aquaporin Interaction Partners. *Biochim. Biophys. Acta* **2013**, https://doi.org/10.1016/j.bbagen.2013.11.012.
[118] Hedfalk, K.; Törnroth-Horsefield, S.; Nyblom, M.; Johanson, U.; Kjellbom, P.; Neutze, R. Aquaporin Gating. *Curr. Opin. Struct. Biol.* **2006**, *16* (4), 447–456, https://doi.org/10.1016/j.sbi.2006.06.009.
[119] Moeller, H. B.; Praetorius, J.; Rutzler, M. R.; Fenton, R. A. Phosphorylation of Aquaporin-2 Regulates Its Endocytosis and Protein-Protein Interactions. *Proc. Natl. Acad. Sci.* **2010**, *107* (1), 424–429, https://doi.org/10.1073/pnas.0910683107.
[120] Zwang, N. A.; Hoffert, J. D.; Pisitkun, T.; Moeller, H. B.; Fenton, R. A.; Knepper, M. A. Identification of Phosphorylation-Dependent Binding Partners of Aquaporin-2 Using Protein Mass Spectrometry. *J. Proteome Res.* **2009**, *8* (3), 1540–1554, https://doi.org/10.1021/pr800894p.
[121] Pisitkun, T.; Shen, R. F.; Knepper, M. A. Identification and Proteomic Profiling of Exosomes in Human Urine. *Proc. Natl. Acad. Sci. U. S. A.* **2004**, *101* (36), 13368–13373, https://doi.org/10.1073/pnas.0403453101.
[122] Noda, Y.; Horikawa, S.; Kanda, E.; Yamashita, M.; Meng, H.; Eto, K.; Li, Y.; Kuwahara, M.; Hirai, K.; Pack, C.; et al. Reciprocal Interaction with G-Actin and Tropomyosin Is Essential for Aquaporin-2 Trafficking. *J. Cell Biol.* **2008**, *182* (3), 587–601, https://doi.org/10.1083/jcb.200709177.
[123] Fields, J. B.; Németh-Cahalan, K. L.; Freites, J. A.; Vorontsova, I.; Hall, J. E.; Tobias, D. J. Calmodulin Gates Aquaporin 0 Permeability through a Positively Charged Cytoplasmic Loop. *J. Biol. Chem.* **2017**, *292* (1), 185–195, https://doi.org/10.1074/jbc.M116.743724.
[124] Ball, L. E.; Garland, D. L.; Crouch, R. K.; Schey, K. L. Post-Translational Modifications of Aquaporin 0 (AQP0) in the Normal Human Lens: Spatial and Temporal Occurrence. *Biochemistry* **2004**, *43* (30), 9856–9865, https://doi.org/10.1021/bi0496034.

Acknowledgements

In the bleak midwinter, as the dreary winds of Lund are howling behind the Kemicentrum windows, I am sitting here in an introspection. I contemplate how all the choices of the past have lead me where I am right now. I feel proud and grateful.

I was privileged to be supervised by you, Susanna. It was from you I learned so much about what it means to be a good scientist. Throughout the entire 5 years in your lab I was constantly mesmerized by your capabilities and your never-ending willingness to help. Especially the last year was a real treat when we got to work close together on writing so much text. Thank you!

Jennifer and Stefan, you were so welcoming when I first arrived in Lund. I will never forget all the fun we had together for example at Tällberg or in Australia. We worked side-by-side for so many years and I missed you very much the last year in the lab.

A dear place in the collection of memories belongs to you, Mike. When things were getting a bit overwhelming I often found inspiration in remembering your working style. Not much can shake you and I admire you for that. This scientific journey all started with you and you prepared me well for a PhD. Thank you!

Here I would also like to express my gratitude to all current and past members of the group. Together we created a such a friendly and fun working atmosphere, that will be hard to beat. Thanks to my collaborators and co-authors of the papers for all your time spent working with common goal. I am also very grateful to all my students, you were my test subjects when I was trying to improve my teaching techniques and your growth gave me a lot of satisfaction.

A big virtual hug goes to all my friends from CMPS, whether still there or already graduated. I had so much fun hanging out with you and having everyday lunch talks and sometimes even fikas. You guys filled my life with joy and made sure I laughed regularly. Thanks to all at the division who have allowed me to learn from them.

Lukas, no words can express how I feel about you, it is beyond gratitude. Describing it is not needed either because I know that you know. Thank you for being here for me to love you this whole time.

Mami, tati, bez Vás bych nikdy nebyla tolik úspěšná. Díky, že jste ze mě vychovali takovou rozumnou, samostatnou a spokojenou bytost!

Structural Details of Human Aquaporin Regulation

VERONIKA NESVEROVA | BIOCHEMISTRY AND STRUCTURAL BIOLOGY | LUND UNIVERSITY